Title

A de novo compound targeting α-synuclein improves deficits in models of Parkinson's disease

Journal

Brain, 139(12)

ISSN

0006-8950

Authors

Wrasidlo, Wolfgang
Tsigelny, Igor F
Price, Diana L
et al.

Publication Date

2016-12-01

DOI

10.1093/brain/aww238

Peer reviewed

doi:10.1093/brain/aww238 BRAIN 2016: 139; 3217–3236 | 3217

BRAIN
A JOURNAL OF NEUROLOGY

A *de novo* compound targeting α-synuclein improves deficits in models of Parkinson's disease

Wolfgang Wrasidlo,[1,*] Igor F. Tsigelny,[1,2,*] Diana L. Price,[3] Garima Dutta,[4] Edward Rockenstein,[1] Thomas C. Schwarz,[5] Karin Ledolter,[5] Douglas Bonhaus,[3] Amy Paulino,[3] Simona Eleuteri,[1] Åge A. Skjevik,[2,6] Valentina L. Kouznetsova,[7] Brian Spencer,[1] Paula Desplats,[1] Tania Gonzalez-Ruelas,[1] Margarita Trejo-Morales,[1] Cassia R. Overk,[1] Stefan Winter,[8] Chunni Zhu,[4] Marie-Francoise Chesselet,[4] Dieter Meier,[3] Herbert Moessler,[8] Robert Konrat[5] and Eliezer Masliah[1,9]

*These authors contributed equally to this work.

Abnormal accumulation and propagation of the neuronal protein α-synuclein has been hypothesized to underlie the pathogenesis of Parkinson's disease, dementia with Lewy bodies and multiple system atrophy. Here we report a *de novo*-developed compound (NPT100-18A) that reduces α-synuclein toxicity through a novel mechanism that involves displacing α-synuclein from the membrane. This compound interacts with a domain in the C-terminus of α-synuclein. The E83R mutation reduces the compound interaction with the 80–90 amino acid region of α-synuclein and prevents the effects of NPT100-18A. *In vitro* studies showed that NPT100-18A reduced the formation of wild-type α-synuclein oligomers in membranes, reduced the neuronal accumulation of α-synuclein, and decreased markers of cell toxicity. *In vivo* studies were conducted in three different α-synuclein transgenic rodent models. Treatment with NPT100-18A ameliorated motor deficits in mThy1 wild-type α-synuclein transgenic mice in a dose-dependent manner at two independent institutions. Neuropathological examination showed that NPT100-18A decreased the accumulation of proteinase K-resistant α-synuclein aggregates in the CNS and was accompanied by the normalization of neuronal and inflammatory markers. These results were confirmed in a mutant line of α-synuclein transgenic mice that is prone to generate oligomers. *In vivo* imaging studies of α-synuclein-GFP transgenic mice using two-photon microscopy showed that NPT100-18A reduced the cortical synaptic accumulation of α-synuclein within 1 h post-administration. Taken together, these studies support the notion that altering the interaction of α-synuclein with the membrane might be a feasible therapeutic approach for developing new disease-modifying treatments of Parkinson's disease and other synucleinopathies.

1 Department of Neuroscience, University of California, San Diego, La Jolla, CA 92093, USA
2 San Diego Supercomputer Center, University of California San Diego, La Jolla, CA 92093, USA
3 Neuropore Therapies, Inc., San Diego, CA 92121, USA
4 Department of Neurology, University of California, Los Angeles, CA, 90095-1769, USA
5 MFPL and University of Vienna, Vienna, Austria
6 Department of Biomedicine, University of Bergen, N-5009 Bergen, Norway
7 Moores Cancer Center, University of California San Diego, La Jolla, CA, 92093, USA
8 EVER Neuropharma, Unterach, Austria
9 Department of Pathology, University of California, San Diego, La Jolla, CA 92093, USA

Received February 12, 2016. Revised June 21, 2016. Accepted August 1, 2016. Advance Access publication September 27, 2016

Correspondence to: Dr Eliezer Masliah,
Department of Neurosciences, University of California, San Diego, La Jolla, CA 92093-0624, USA
E-mail: emasliah@UCSD.edu

Keywords: alpha-synuclein; Parkinson's disease; experimental models; cellular mechanisms; synucleinopathy

Abbreviations: DEST = dark-state exchange saturation transfer; POPG = 1-palmitoyl-2-oleoyl-sn-glycero-3-phosphoglycerol; NMR = nuclear magnetic resonance; UCLA = University of California Los Angeles; UCSD = University of California San Diego

Introduction

Progressive accumulation of the synaptic protein α-synuclein (encoded by *SNCA*) is proposed to have a critical role in the pathogenesis of Parkinson's disease, dementia with Lewy bodies and multiple system atrophy, jointly denominated synucleinopathies (Spillantini *et al.*, 1997; Wakabayashi *et al.*, 1998; McKeith *et al.*, 2005). Approximately 10 million people worldwide are affected by synucleinopathies, and currently no disease-modifying therapy is available. The precise mechanisms resulting in pathological accumulation of α-synuclein are not fully understood; however, evidence suggests that alterations in the rate of synthesis (Farrer *et al.*, 2001; Singleton *et al.*, 2003, 2013; Tan and Skipper, 2007; Fujioka *et al.*, 2014), aggregation (Polymeropoulos *et al.*, 1997; Kruger *et al.*, 1998; Lashuel *et al.*, 2002), and clearance might be involved (Crews *et al.*, 2010; Dehay *et al.*, 2013; Xilouri *et al.*, 2016).

α-Synuclein accumulation is proposed to lead to neurodegeneration via the formation of toxic oligomers (Lashuel *et al.*, 2013) with possible prion-like propagation from cell-to-cell (Brundin *et al.*, 2010; Lee *et al.*, 2010; Luk *et al.*, 2012). α-Synuclein oligomers, varying widely in size, shape and conformation, might contribute to neurodegeneration. Some studies propose that small- or intermediate-sized oligomers are toxic (Conway *et al.*, 2000), while other studies suggest that larger molecular weight aggregates are involved (Bucciantini *et al.*, 2002; Cremades *et al.*, 2012). An alternative explanation has been that free α-synuclein, not organized as a tetramer, might be toxic (Bartels *et al.*, 2011).

Supporting the possibility that higher-order α-synuclein aggregates are toxic, molecular dynamic simulation and biophysical studies provided evidence that α-synuclein binding and subsequent penetration of the neuronal membrane are important events in this process (Bortolus *et al.*, 2008; Tsigelny *et al.*, 2008; van Rooijen *et al.*, 2010). Thus, interactions between α-synuclein and lipids in the neuronal cell membrane are proposed as an important step in the process of oligomerization and cytotoxicity (Beyer, 2007; Tsigelny *et al.*, 2012). Therefore strategies directed at displacing α-synuclein from the membrane, increasing degradation and clearance, preventing aggregation, or decreasing α-synuclein synthesis might represent reasonable therapeutic strategies.

Previous studies have targeted α-synuclein aggregates by means of antibodies (Games *et al.*, 2013), proteolytic enzymes (Spencer *et al.*, 2013) and with small molecules (Toth *et al.*, 2014) that decrease α-synuclein aggregation or fibrillation. Using computational analysis, we showed that formation of α-synuclein propagating dimers in the membrane is an early step in the development of toxic α-synuclein oligomers (Tsigelny *et al.*, 2008, 2012) and that targeting the C-terminus of α-synuclein with peptidomimetic compounds might be therapeutically relevant. We have recently synthesized a library of 34 peptidomimetic analogues targeting α-synuclein and identified NPT100-18A as the most promising (Patent #8,450,481). Here we investigated the therapeutic potential of these novel cyclic peptidomimetic compounds with a pirimido-pyrazine scaffold by *in silico* and biophysical methods. NPT100-18A is proposed to potentially interact with α-synuclein in the membrane and reducing toxic oligomer formation. Cell-based and *in vivo* experiments in three different α-synuclein transgenic models showed that NPT100-18A ameliorated behavioural deficits and neurodegeneration supporting the possibility that targeting the early process of α-synuclein oligomerization on the membrane might be a viable therapeutic approach for synucleinopathies.

Material and methods

Further details and full protocols can be found in the Supplementary material.

Chemical synthesis of NPT100-18A

Briefly, NPT100-18A was developed *de novo* by molecular modelling methods targeting a C-terminus domain of α-synuclein, which is important for dimerization and membrane penetration (Fig. 1). NPT100-18A is a cyclic peptidomimetic compound with a pirimido-pyrazine scaffold that was derived from small peptides (e.g. KKDQLGK) analogous to the 96–102 domain of α-synuclein (Patent #8,450,481). A complete description of the design and synthesis is provided in the Supplementary material.

α-Synuclein pharmacophore modelling and NPT100-18A docking

Formation of α-synuclein propagating dimers in the membrane is an early step in the generation of toxic α-synuclein oligomers, and interactions between a domain in residues

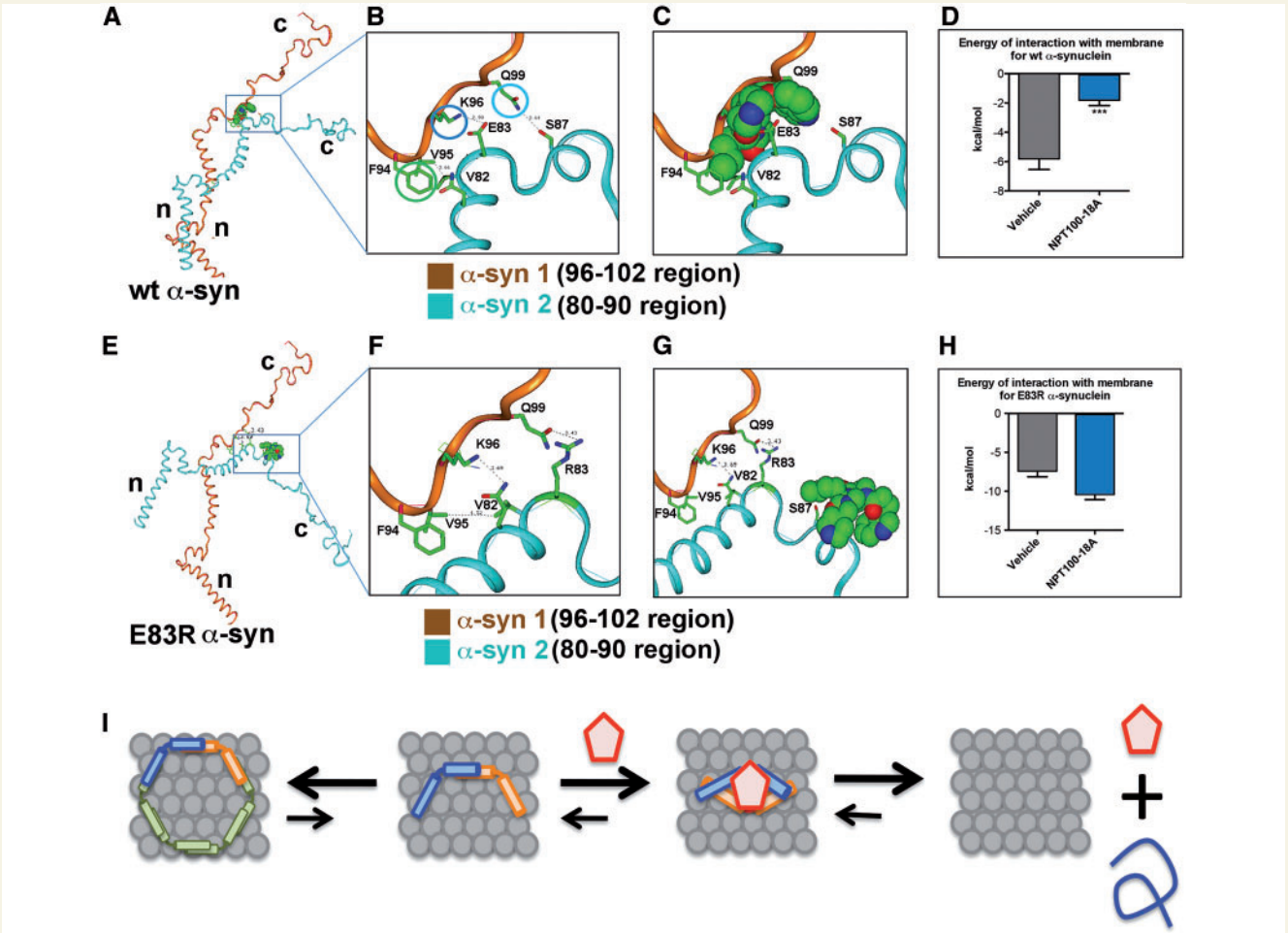

Figure 1 Molecular dynamics modelling studies of the mechanisms of NPT100–18A interactions with α-synuclein in lipid membranes. (**A**) Frequent place of binding of NPT100–18A. The compound mimics one of the regions of α-synuclein that most frequently binds to anther α-synuclein molecule during oligomerization leading to annular structures. (**B**) Close-up of the region in **A**. Residues interacting between the neighbouring α-synuclein molecules in the dimer that propagates to an annular oligomer. (**C**) Close-up of the region in **A** and **B**. The NPT100-18A is presented as a space-filling model with the atoms colour-coded by the type: red, oxygen; blue, nitrogen; green, carbon. (**D**) Energies of interaction for the membrane and α-synuclein dimers are significantly less favourable in the presence of NPT100-18A indicating that α-synuclein was less likely to propagate to annular structures. (**E**) Frequent binding location for NPT100–18A on the E83R α-synuclein mutant. In this case the mutation most likely alters the α-synuclein molecule, which resulted in abolishment of compound activity. (**F**) Magnification of residues that interacts between the mutant α-synuclein molecules. (**G**) Frequent position of the compound on the α-synuclein molecule. (**H**) Energies of interaction with the membrane of α-synuclein dimers that propagate to higher oligomers did not diminish despite compound binding. (**I**) Scheme of the compound function. The dimers and trimers created on the surface of the membrane can propagate to the annular structures or in the presence of the compound (red pentagon) the α-synuclein conformation changed effecting the formation of dimers and trimers in the membrane. ***$P < 0.01$ by Student *t*-test. wt = wild-type.

96–102 in one α-synuclein and 80–90 in the parent α-synuclein are important in this process (Tsigelny *et al.*, 2008, 2012). Using this model, we predicted that docking a cyclic peptidomimetic molecule in between the sites of interaction of the α-synuclein monomers forming the propagating dimer would interfere the formation of toxic α-synuclein species (Patent #8,450,481). Molecular dynamic simulation studies were performed to characterize the possible binding position of NPT100-18A and analogues within wild-type or mutant α-synuclein dimers and to examine the effects of these interactions with the ability of α-synuclein to bind the membrane and form propagating dimers and oligomers.

Synthesis of wild-type and E83R mutant α-synuclein

Recombinant human α-synuclein was used for the nuclear magnetic resonance (NMR) and cell free immunoblot studies. *Escherichia coli* BL21 heat competent cells were transformed with wild-type human α-synuclein and E83R.

Nuclear magnetic resonance studies of NPT100-18A interactions with micelle-bound α-synuclein

NMR spectra were recorded on Varian Inova 800 MHz and Bruker Avance 800 MHz spectrometers with 10% D_2O as lock solvent. Spectra were processed using NMR Pipe (Delaglio *et al.*, 1995). All measurements were carried out at pH 6.5 and 35°C with a protein concentration of 0.4 mM and 0.4 mg/ml POPG (1-palmitoyl-2-oleoyl-sn-glycero-3-phosphoglycerol). ^{1}H-^{15}N correlation spectra were recorded with Rance-Kay detected sensitivity enhanced heteronuclear single quantum coherence (HSQCS) (Cavanagh *et al.*, 1991; Kay *et al.*, 1992).

Neuronal cells, lentiviral vectors and treatments

The lentivirus wild-type α-synuclein vector (LV-wt-α-syn) was previously characterized (Bar-On *et al.*, 2008). LV-α-syn E83R was prepared by site-directed polymerase chain reaction (PCR) mutagenesis (Agilent Technologies). Lentiviruses were packaged by transient transfection of the three packaging plasmids and the vector plasmid in 293 T cells, as previously described (Tiscornia *et al.*, 2006; Spencer *et al.*, 2009). Primary neuronal cells (cortical, mouse, embryonic Day 18) were used for the *in vitro* experiments (Eleuteri *et al.*, 2015).

Preparation of *in vitro* cell-free α-synuclein aggregates with artificial lipid membranes and electron microscopy analysis

A synthetic lipid monolayer was generated as described (Ford *et al.*, 2001). Briefly, 56cholesterol, phosphatidylethanolamine and phosphatidylcholine (all from Sigma-Aldrich) were dissolved in chloroform at a concentration of 10 mg/ml. Phosphatidylinositol-4,5-biphosphate (Sigma-Aldrich) was dissolved at 1 mg/ml in 3:1 chloroform:methanol.

Animals and treatments

University of California San Diego (UCSD) and University of California Los Angeles (UCLA) are IACUC accredited institutions and the Animal Subjects Committee at each institution approved the experimental protocol followed in all studies according to the AAALAC International guidelines. At UCSD, all behavioural testing procedures were performed under UCSD IACUC Protocol S02221. The following α-synuclein transgenic mouse lines were used: (i) mThy1-wt-α-syn transgenic (line 61); (ii) mThy1-E57K-α-syn transgenic (line 16); and (iii) PDGFβ-wt-α-syn-GFP (line 78) transgenic mice. Additional information about each animal line as well as initial behavioural and dose-finding studies is provided in the Supplementary material.

Pharmacokinetic studies

Pharmacokinetic studies to determine the plasma and brain distribution of NPT100-18A were performed after acute intravenous injections at one of five doses (0.1, 1, 5, 10, 20 mg/kg, intravenously) and 20 mg/kg intraperitoneally (SAI-Life Sciences). Three mice per group per time point (0, 0.08, 0.25, 0.5, 1, 2, 4, 8, 24, and 48 h) were assessed for a total of 150 mice.

Behavioural testing

At UCSD, round beam data were collected using a custom built apparatus consisting of two removable Delrin® acetal plastic rods (3 and 1 cm diameter) on a smooth acrylic frame elevated 17.5 to 22.5 cm above a testing bench.

Reproducibility study at UCLA

Studies at UCLA were performed under IACUC protocol 1996-092. In agreement with the studies at UCSD, mThy1-α-syn transgenic and non-transgenic littermate mice (3 months old, males) were used. Studies at UCLA included evaluations on the challenging beam traversal test and an open field locomotor assessment.

Real-time polymerase chain reaction analysis

Total RNA was isolated from mice brains using the RNeasy® Lipid mini kit (Qiagen) and was reverse transcribed using RT^2 First Strand kit (Qiagen) from 1 μg of total RNA. Real-time PCR analysis was performed using the StepOnePlus™ real-time PCR system (Applied Biosystems).

Two-photon live imaging of synapses in α-synuclein-GFP transgenic mice

For these experiments the PDGF-α-syn-GFP transgenic mouse model was used. A total of 12 transgenic male mice (6 months of age, $n = 6$ vehicle and $n = 6$ NPT100-18A) were used.

Immunoblot analysis of α-synuclein

As previously described, neuronal cell lysates or brains were homogenized and divided into cytosolic and particulate (membrane) fractions (Spencer *et al.*, 2009; Crews *et al.*, 2010).

Immunocytochemical and neuropathological analysis

Analysis of α-synuclein accumulation was performed in serially sectioned, free-floating vibratome sections.

Image analysis and stereology

Sections immunostained with antibodies against α-synuclein, TH, and GFAP were analysed with a digital Olympus bright field digital microscope (BX41). For each case a total of three sections (four digital images per section at 400× magnification) were obtained from the neocortex, striatum and hippocampus and analysed as previously described with the ImageJ program (NIH) to obtain optical density, levels were corrected to background.

Double immunolabelling and confocal microscopy analysis

To determine the co-localization between CT-α-syn and the synaptic marker synaptophysin (SY38) or the neurofilament marker SMI312, double-labelling experiments were performed as previously described (Spencer *et al.*, 2009).

Electron microscopy and immunogold analysis

Vibratome sections from the non-transgenic and α-synuclein transgenic mice were post-fixed in 1% glutaraldehyde, treated with osmium tetroxide, embedded in Epon® araldite for ultramicrotome sectioning and electron microscopy (Masliah *et al.*, 2011).

Data processing and statistical analysis

Raw data from the behavioural tests were recorded by hand and then entered into MS Excel for subsequent analysis and graphing using GraphPad Prism (GraphPad Software, Inc., La Jolla, CA). The dependent measures for performance on each assay were determined for each animal and presented as the mean ± the standard error of the mean (SEM). Group means were determined for each measure and analysed by either a one-way ANOVA, regular or repeated measure followed by *post hoc* comparisons using Dunnett's or Tukey's multiple comparisons tests, as appropriate. The criterion for statistical significance was $P < 0.05$.

Results

Molecular modelling studies of NPT100-18A docking to α-synuclein dimer

Previous studies showed that α-synuclein oligomerization could be initiated by dimerization on membrane surfaces. Further molecular dynamic studies suggest that interactions between amino acids (aa) 96–102 of one α-synuclein molecule with aa 80–90 of the complementary α-synuclein molecule are important in this process. Using this information on the 96–102 β-turn domain region, we developed a pharmacophore model for designing small molecule peptidomimetics that can interact with this domain. This pharmacophore in the 96–102 region has five distinct docking centres including four that are electrostatic and one hydrophobic in nature (Supplementary Fig. 1C). This 96–102 amino acid region represents a β-turn domain and is important as a recognition motif for protein interactions. Next, we designed 34 compounds (Supplementary Fig. 1B) that were docked into the five docking centres of the pharmacophore model to assess the geometric and molecular interactions of each of the analogues. Compared to the other 33 analogues, NPT100-18A had the closest fit to each docking centre. Further molecular dynamic simulations showed that NPT100-18A also interacted most frequently with residues 81 (Thr), 82 (Val) and 83 (Glu) (Supplementary Fig. 1E) of the α-synuclein dimerization partner. The active centres of the compound mimic the corresponding residues of α-synuclein C-terminus domain (Fig. 1B) and prevented the formation of the dimer and membrane interactions (Fig. 1D).

Further confirmation of the pharmacophore model (Supplementary Fig. 1C) was obtained by the use of the ICM (Molsof) software that identifies binding pockets. Using ICM software, we confirmed that the 96–102 aa region of α-synuclein constituted a binding pocket (Supplementary Fig. 2A–C). For each of the 34 analogues, three values were generated, first a score for the degree of interaction with the pocket (based on the ICM generated binding model) and second the polar surface area and partition coefficient (logP) (Supplementary Fig. 2D). Compared to the other 33 analogues, NPT100-18A had the most favourable score (−3.57), polar surface area (84), and logP (4.32) (Supplementary Fig. 2D).

To further validate our model, we identified mutations in the aa 96–102 pharmacophore region and in the dimerization neighbour region aa 80–90, which allowed dimerization but affected NPT100-18A interactions. Using molecular dynamic simulations we found that mutations in the 96–102 aa region destabilized α-synuclein in such a way that will disrupt dimerization, therefore mutations on the 80–90 regions were considered a better choice because the mutations caused the least structural changes in conformation. Using molecular dynamic simulations we found that the α-synuclein (E83R) mutation abrogated the formation of the H-bond between NPT100-18A and the C-terminus of α-synuclein (Fig. 1E–G). As expected, this mutation led to a shift in the docking site of NPT100-18A from the E83R position to residues 90, 92, 93 (Fig. 1E–G). In this new location, NPT100-18A was outside of the interface of interaction between two α-synucleins in the heterodimer and therefore the compound was unable to interfere with the process of oligomerization. Unlike the wild-type α-synuclein (Fig. 1D), the energy of interaction for E83R with the membrane was undiminished (Fig. 1H). Taken together, the molecular dynamic simulation results suggest that NPT100-18A interactions with the C-

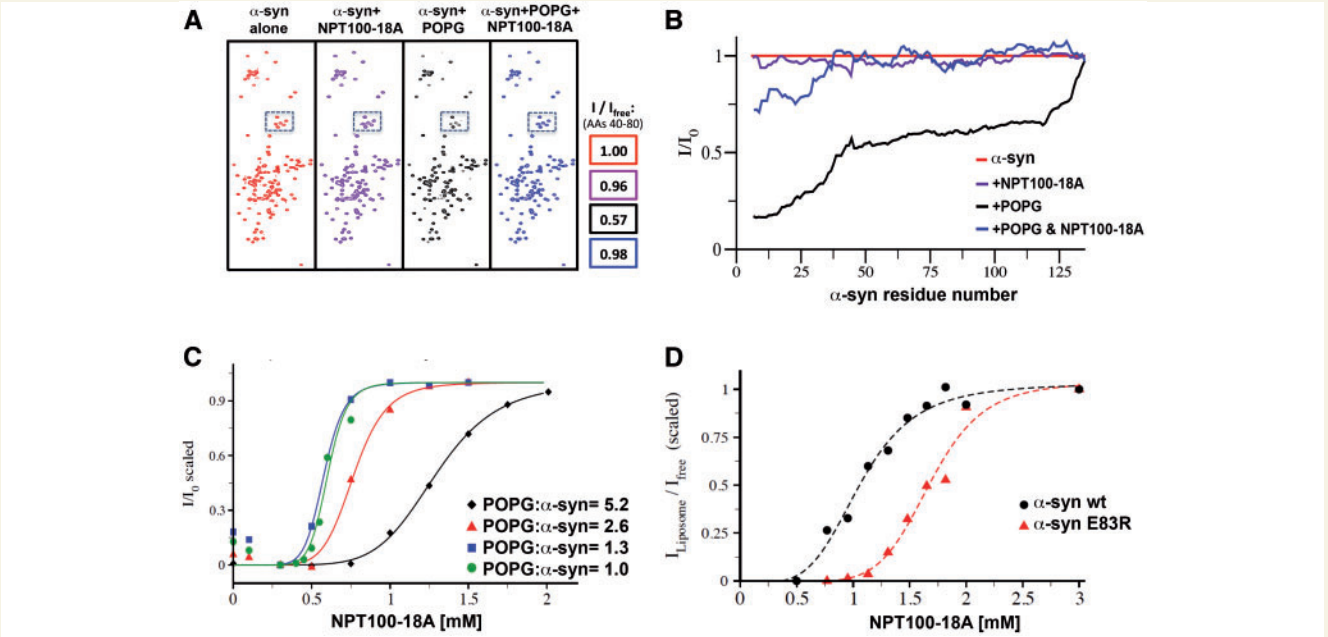

Figure 2 HSQC-based NMR characterization of the effects of NPT100-18A on α-synuclein lipid binding. (**A**) Series of HSQC spectra demonstrating that the addition of NPT100-18A (purple) to free α-synuclein (red) does not change the spectrum, while addition of liposomes (black) leads to a signal reduction that can be reversed by NPT100-18A (blue); the number in the box to the right represents the mean for each spectra. (**B**) Analysis of signal intensity for the spectra of free- and liposome-bound α-synuclein in the presence or absence of NPT100-18A. (**C**) NPT100-18A concentration dependence of liposome displacement for α-synuclein compared at different POPG:α-synuclein ratios. A clear shift towards lower apparent Kd values and more sigmoidality (cooperativity) can be seen when the POPG:α-synuclein ratio is decreased (higher local α-synuclein concentration on the membrane and thus more pronounced α-synuclein oligomer formation). The blue and green curves were recorded at the same ratio, while the total concentration was doubled in the green curve. This excludes the possibility of POPG concentration dependence (lines are fits with the Hill equation performed as a guide). All measurements apart from green with 200 μM α-synuclein, POPG concentrations were 0.8 mg/ml, 0.4 mg/ml and 0.2 mg/ml for black, red and blue, respectively (pH = 6.5). (**D**) NPT100-18A concentration dependence of liposome displacement for wild-type α-synuclein and the mutant E83R. Increasing concentration of NPT100-18A leads to more displacement of α-synuclein from the liposome (observed as an increase in signal intensity). Here the average value of the relative signal intensities from available resolved residues in the region 40–90 was plotted against the ligand concentration. The strong difference between wild-type (wt) and mutant (E83) in response to the ligand can easily be observed (dashed lines are fits with the Hill equation performed as a guide only).

terminus of α-synuclein might reduce oligomerization by interfering with membrane binding and dimer formation (Fig. 1I).

NMR studies show that NPT100-18A might reduce α-synuclein interactions with the liposome

To investigate further the effects of NPT100-18A on the ability of α-synuclein to bind membranes, NMR studies were performed with liposome-bound and free ^{15}N-^{1}H-labelled α-synuclein in the presence or absence of NPT100-18A (Fig. 2A). Addition of liposomes to α-synuclein led to a drastic loss in signal intensities, while shifts were unaffected (Fig. 2A and Supplementary Fig. 3A). Given the large size of the liposomes, only the free state of α-synuclein can be observed. Thus only the observable free-form of α-synuclein was used to calculate the populations of free and bound α-synuclein, respectively. NMR studies were performed with ^{15}N-^{1}H α-synuclein for different experimental conditions. While with free α-synuclein (Fig. 2A and B) no changes in signal intensity were detected, when adding NTP100-18A (Fig 2A and B), the α-synuclein signal was reduced in the presence of lipid (Fig. 2A and B) and the intensity of the signal recovered when adding NPT100-18A (Fig 2A and B). Increasing NPT100-18A concentrations led to wild-type α-synuclein signal recovery when mixed with lipids at various ratios (Fig. 2C). At high concentrations NTP100-18A led to complete release of α-synuclein from the membrane. Interestingly, the apparent activity of NTP100-18A critically depended on the liposome/α-synuclein ratio. At a lower ratio (POPG:α-syn = 1.3) the NTP100-18A-induced release of α-synuclein was more efficient than at higher ratios (POPG:α-syn = 8.7). These results suggest that NTP100-18A does not bind to monomeric, soluble α-synuclein but releases α-synuclein from the liposome vesicles at high ligand concentrations. To rule out possible liposome

disruption in the presence of NPT100-18A, dynamic light scattering measurements were performed. Dynamic light scattering unambiguously indicated that liposomes were not disrupted by NPT100-18A (data not shown). Thus, the recovery of signal intensity with NPT100-18A might be related to the potential release of α-synuclein from the liposome surface. To further investigate this possibility, the differential effects of NPT100-18A were analysed by NMR using wild-type and mutant α-synuclein (E83R) in the presence of liposomes. This was based on the molecular dynamic simulations that suggested that compared to wild-type α-synuclein, NPT100-18A might be less effective at releasing the mutant α-synuclein (E83R) from the lipid membrane. The NMR analysis confirmed the spectral difference between α-synuclein alone and in the presence of POPG (Supplementary Fig. 3A) and wild-type and mutant α-synuclein (E83R) (Supplementary Fig. 3B). Moreover the NMR studies showed that at low concentrations, NPT100-18A was more effective at displacing wild-type α-synuclein from the liposomes than mutant α-synuclein (E83R) (Fig. 2D); however, at the highest concentrations NPT100-18A has similar effects on wild-type and mutant α-synuclein (E83R) (Fig. 2D).

Further analysis of the membrane-bound state of α-synuclein and its dependence on NPT100-18A binding was probed by using dark-state exchange saturation transfer (DEST) NMR methodology. The DEST methodology probes the equilibrium between NMR visible (detectable) and invisible (undetectable) states of proteins. Typically proteins that are transiently bound to high-molecular weight complexes show pronounced line-broadening effects (Supplementary Fig. 4A). The attenuation profile provides information about the bound state at a residue-specific resolution, whereby the level of attenuation depends on residual dynamics in the bound state (Supplementary Fig. 4A).

To probe the effect of NPT100-18A on the membrane-bound state of α-synuclein DEST and heteronuclear single quantum coherence (HSQC) NMR experiments were performed using ligand concentrations that did not release from the liposomes (α-synuclein: 400 μM; NTP100-18A: 300 μM). While the HSQC shows and quantifies the population of the bound α-synuclein species (Supplementary Fig. 4B), the DEST profile shows both the population and residual structural dynamics of the bound state (Supplementary Fig. 4B). Analysis of effects of NPT100-18A on α-synuclein in the presence of liposomes shows by HSQC (top, black) and DEST (bottom, red) differences in the membrane-bound state of α-synuclein before and after addition of 300 μM NTP100-18A (prior to the displacement from the membrane) (Supplementary Fig. 4C). Interestingly, HSQC peak intensity decreased after adding 300 μM NPT100-18A, while the DEST measurement shows a slight increase on a per residue basis (Supplementary Fig. 4D) targeting the intermediate to c-terminus portion of α-synuclein between aa 80–102. Based on the NTP100-18A HSQC data at 300 μM there is still α-synuclein bound to membrane. In contrast, the DEST structural dynamics of membrane-bound α-synuclein is clearly altered, suggesting a change in the molecular interactions of α-synuclein.

In conclusion, the NMR data provide evidence that NPT100-18A might interact among others with the C-terminus region of α-synuclein (80–90 and 96–102). Most importantly, these changes of the interaction interface could be detected at concentrations where no release of α-synuclein from the liposomes was observed (Supplementary Fig. 4C and D). It was only at higher concentrations that α-synuclein was released from the membrane and existed in a monomeric form in solution, which had no measureable affinity to the ligand (Fig. 2C and D). Therefore, the potential mode of action of NPT100-18A is to interfere with the membrane-bound state of α-synuclein and alter its conformational ensemble accompanied by attenuation of its membrane-induced aggregation into oligomers.

NPT100-18A reduces α-synuclein oligomer formation in lipid membranes and neurotoxicity

Given that the molecular modelling (Fig. 1) and NMR (Fig. 2) studies indicated that NPT100-18A enhances α-synuclein displacement from the membrane, next we investigated the effects of NPT100-18A on α-synuclein aggregation in a lipid matrix where synthetic membrane preparations with negative staining were evaluated by electron microscopy. Under baseline conditions, ring-like α-synuclein oligomers were detected on the prepared synthetic membranes within the 12 h incubation period, and addition of NPT100-18A diminished the formation of ring oligomers by 60% when wild-type α-synuclein was used (Fig. 3A and B); however, no effect was detected with mutant α-synuclein E83R (Fig. 3C and D). Electron microscopy immunogold experiments confirmed that the ring-like structures in the membranes consisted of anti-α-synuclein immunogold-decorated particles; NPT100-18A reduced the formation of such gold-bearing annular α-synuclein (Fig. 3E and F). In comparison, similar immunogold experiments showed that NPT100-18A had no effect on the formation of annular oligomers when mutant α-synuclein E83R was used (Fig. 3G and H).

Next, we investigated the effects of NPT100-18A in primary neuronal cells infected with lentivirus expressing either wild-type or E83R α-synuclein. Lentiviral expression resulted in abnormal accumulation of wild-type and E83R α-synuclein in primary neuronal cultures, which was distributed both in the neuronal cell bodies and extended to neuritic processes (Fig. 3I and J). Treatment with NPT100-18A considerably reduced the accumulation of wild-type α-synuclein in the neuronal cell processes (Fig. 3I and J), but not in E83R α-synuclein (Fig. 3I and J). Using Scholl analysis, confocal imaging showed that neuronal cells over-expressing α-synuclein displayed reduced length of

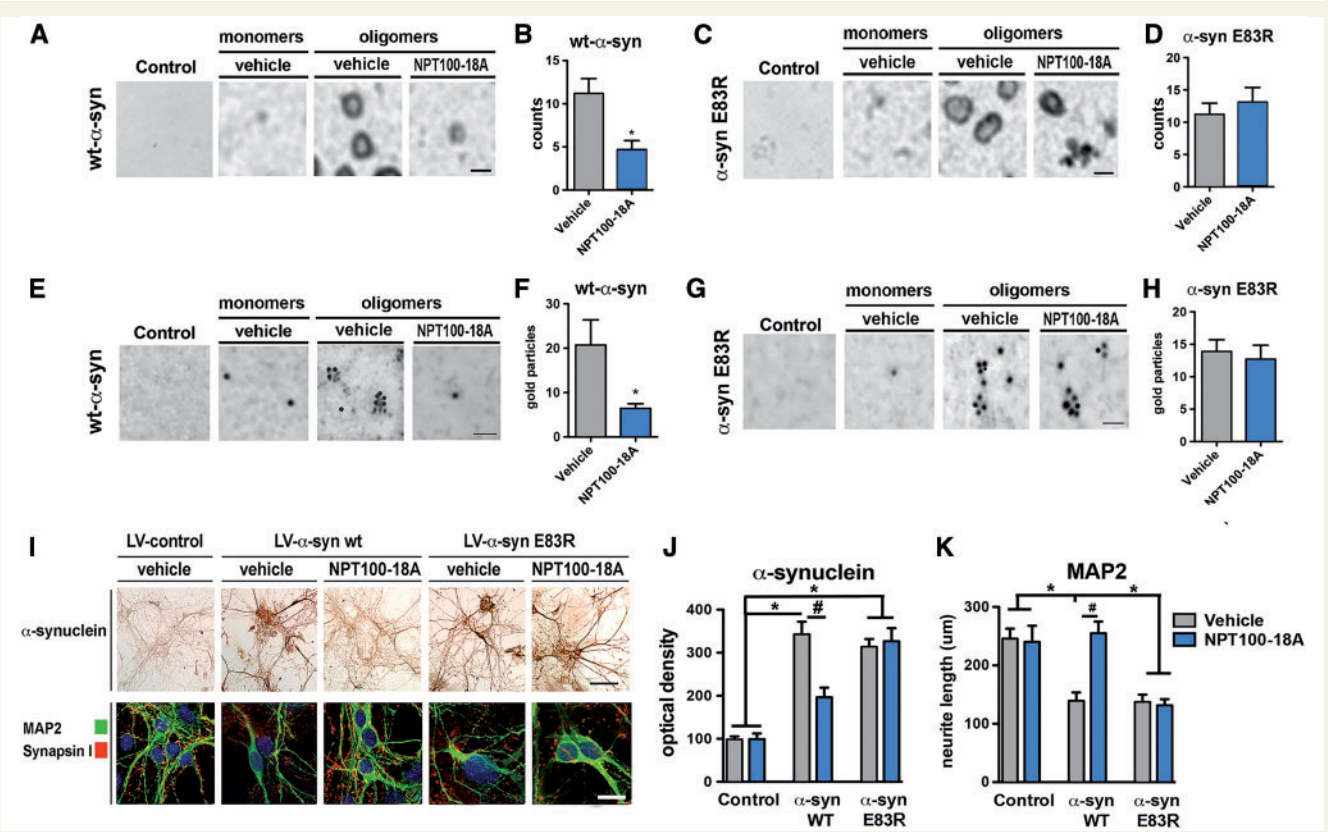

Figure 3 ***In vitro*** **analysis of the effects of NPT100-18A on α-synuclein oligomerization and toxicity.** (**A**) Electron microscopic analysis of the effects of NPT100-18A (2 μM) on the formation of ring-like wild-type α-synuclein oligomers in a lipid membrane matrix. (**B**) Computer aided image analysis showing that NPT100-18A reduces ring-like oligomers with wild-type α-synuclein. (**C**) Electron microscopic analysis of the effects of NPT100-18A on E83R α-synuclein in a lipid membrane matrix. (**D**) Computer aided image analysis showing that NPT100-18A does not reduce ring-like E83R α-synuclein oligomers. (**E**) Immunogold (10 nm) electron microscopic analysis with a monoclonal antibody against human α-synuclein to evaluate the effects of NPT100-18A of the formation of ring-like wild-type α-synuclein oligomers in a lipid membrane matrix. (**F**) NPT100-18A significantly reduced the number of gold particles $^{*}P < 0.05$ versus vehicle-treated α-synuclein wild-type group by Student *t*-test. (**G**) Immunogold electron microscopic analysis with a monoclonal antibody against human α-synuclein to evaluate the effects of NPT100-18A of the formation of ring-like E83R α-synuclein oligomers in a lipid membrane matrix. (**H**) NPT100-18A did not affect the number of gold particles. (**I**) Primary neuronal cultures from rat (embryonic Day 18) neocortex were infected with LV-control, LV-wild-type or E83R α-synuclein and treated with NPT100-18A at 1 μM. Cells in the *upper row* were immunostained with an antibody against α-synuclein and developed with diaminobenzidine. Cells in the lower panel were double labelled with antibodies against synapsin-1 and MAP2 and imaged with the laser scanning confocal microscope. (**J**) Computer aided analysis of levels of α-synuclein showing increased immunoreactivity in cells infected with wild-type and E83R α-synuclein. Compared to vehicle, treatment with NPT100-18A reduced the accumulation of wild-type but not E83R α-synuclein in primary neurons. (**K**) Computer aided Scholl image analysis of the length of MAP2 immunoreactive neurites showing decreased neurite lengths in cells infected with wild-type and E83R α-synuclein. Treatment with NPT100-18A recovered neuritic length in cells expressing wild-type but not E83R α-synuclein. Statistical analysis for **A–H** performed using Student *t*-test, $^{*}P < 0.05$. Statistical analysis for **J–K** performed using one-way ANOVA, $^{*}P < 0.05$ versus vehicle-treated control group using Dunnett's *post hoc* comparison and $^{\#}P < 0.05$ versus vehicle-treated α-synuclein cells using Tukey-Kramer *post hoc* comparison; error bars are SEM; three replicates per group. Scale bar in **A**, **C**, **E** and **G** = 100 Å; **I** = 10 μm.

neuronal processes. Moreover, the number of synapsin-I-positive punctae was reduced (Fig. 3I). Treatment with NPT100-18A normalized the appearance and length of neurites and the synapsin-I deficits in neuronal cells expressing wild-type α-synuclein (Fig. 3I and K), but not in neuronal cells expressing E83R α-synuclein (Fig. 3I and K). Immunoblot analysis using primary neuronal cells infected with LV-control, LV-wt-α-syn, or LV-E83R-α-syn was performed to complement the immunocytochemical experiments. Western blot analysis using Syn211 antibody (Supplementary Fig. 5A–C) found NPT-treatment significant decreased oligomeric wild-type α-synuclein, but not E83R α-synuclein, whereas monomeric α-synuclein was not affected. Dot blot analysis using A11 antibody (Supplementary Fig. 5D–F) further confirmed a reduction in wild-type α-synuclein, but not E83R α-synuclein. Taken together these results confirm that NPT100-18A alters wild-type α-synuclein, but not E83R α-synuclein, and its effects are on oligomeric aggregation, but not monomeric α-synuclein.

Independent studies confirms NPT100-18A improves motor behavioural deficits in mThy1-α-syn wild-type transgenic mice

NPT100-18A exposure levels in plasma and brain were analysed in wild-type mice at 10 time points. The 20 mg/kg dose was detected in plasma up to 24 h (Supplementary Fig. 6A and B). Following intravenous administration, NPT100-18A exhibited rapid brain migration as indicated by T_{max} in range of 0.08–0.25 h at doses of 1, 5, 10, 15, and 20 mg/kg (Supplementary Fig. 6C). Brain-to-plasma exposure (last measurable area under the curve, AUC_{last}) ratio was between 0.5% at the lowest dose and 11% at the higher doses (Supplementary Fig. 6B and C). The mean concentration of drug in the brain was 250 ng/ml, which equals ~500 nM. Similar pharmacokinetic studies were performed following intraperitoneal administration of NPT100-18A at 20 mg/kg. These studies showed a brain-to-plasma exposure ratio of 8%, plasma concentrations declined monoexponetially with an AUC_{last} at 24 h, and brain concentrations declined exponentially with an AUC_{last} at 4 h. Following intraperitoneal administration, NPT 100-18A exhibited a rapid migration to the brain with a T_{max} of 0.08 h.

We investigated the effects of NPT100-18A on motor behavioural performance deficits present in mThy-1-α-syn transgenic mice at UCSD (Fig. 4A and B) and at UCLA (Fig. 4C–F). Mice at both sites were treated once daily for 3 months with an intraperitoneal injection of 1, 5, 10 or 20 mg/kg with behavioural testing starting on Day 70 of 90. This transgenic mouse model develops Parkinson's disease-like motor and non-motor deficits as well as neuropathological indices (including α-synuclein aggregates, alterations in markers associated with neurodegeneration, and decreases in synaptic markers) starting at 3 months of age. In motor behavioural assessments conducted at UCSD, vehicle-treated α-synuclein transgenic mice displayed deficits in the horizontal round beam test; treatment with NPT100-18A (10 and 20 mg/kg) reduced the number of errors (foot slips) (Fig. 4A). In the open field, vehicle-treated α-synuclein transgenic mice displayed increased total activity compared to vehicle-treated non-transgenic mice (Fig. 4B); however, there were no statistically significant effects in α-synuclein mice treated with NPT100-18A (Fig. 4B).

An independent study was performed at UCLA to confirm the effects of NPT100-18A administration on motor performance deficits in α-synuclein transgenic mice. A challenging beam apparatus was used instead of a round beam to evaluate the effects of NPT100-18A on motor performance in mThy1-α-syn mice. Vehicle-treated α-synuclein transgenic mice had statistically significant deficits in motor performance in the challenging beam and open field assessment (Fig. 4C–F). Consistent with the round beam results at UCSD, the study at UCLA showed that NPT100-18A (10 mg/kg) treatment of α-synuclein transgenic mice decreased the error rates on the challenging beam at 4.4 and 6.2 months of age (1 and 3 months of treatment, respectively) (Fig. 4C). Analysis of challenging beam performance at 4.4 months of age by trial with paired comparisons demonstrated a statistically significant reduction in errors per step during three of five trials (Fig. 4D). Treatment restored habituation in the open field in the third 5 min time bin compared to the impaired vehicle-treated α-synuclein transgenic (Fig. 4E and F). Taken together, two independent efficacy evaluations of NPT100-18A administration confirmed beneficial effects on motor performance deficits present in an α-synuclein transgenic mouse model of Parkinson's disease/dementia with Lewy bodies.

NPT100-18A decreases the accumulation of α-synuclein in transgenic mice

Given that the most significant effects on motor performance were detected at the higher doses, subsequent neuropathological and immunoblot studies were performed in animals treated at 10 and 20 mg/kg. Results presented below are from the 20 mg/kg group unless otherwise noted. Compared to non-transgenic mice, there were abundant accumulations of α-synuclein in neurons and neuropil in the neocortex of vehicle-treated α-synuclein transgenic mice (Fig. 5A and B), hippocampus (Fig. 5A and C), striatum (Fig. 5A and D), and substantia nigra (Fig. 5A and E). Treatment with NPT100-18A significantly reduced the accumulation of α-synuclein in the neuropil in the neocortex (Fig. 5A and B), hippocampus (Fig. 5A and C) and striatum (Fig. 5A and D) but not substantia nigra (Fig. 5A and E). By immunoblot, NPT100-18A reduced the accumulation of α-synuclein oligomers in sodium dodecyl sulphate (SDS) (Fig. 5F, H and I) and monomers were unchanged (Fig. 5F and G). Moreover, analysis of fractioned tissues from the vehicle-treated α-synuclein transgenic mice revealed increased accumulation of α-synuclein in the membrane fraction as opposed to the cytosolic fraction (Fig. 5J). Treatment with NPT100-18A resulted in decreased accumulation of α-synuclein in the membrane and increased cytosolic α-synuclein (Fig. 5J and K), as demonstrated with a polyclonal antibody against α-synuclein, as well as reduced α-synuclein accumulation in native gels (Fig. 5L).

We have previously shown that aggregated neurotoxic α-synuclein can be detected with the SYN105 antibody against truncated C-terminus α-synuclein (Games *et al.*, 2013). There was extensive accumulation of α-synuclein in the synapses and axonal processes in the vehicle-treated α-synuclein transgenic mice in the neocortex, hippocampus and striatum of α-synuclein transgenic mice (Supplementary Fig. 7A), which NPT100-18A treatment significantly reduce in the axons (Supplementary Fig. 7A and B). This was

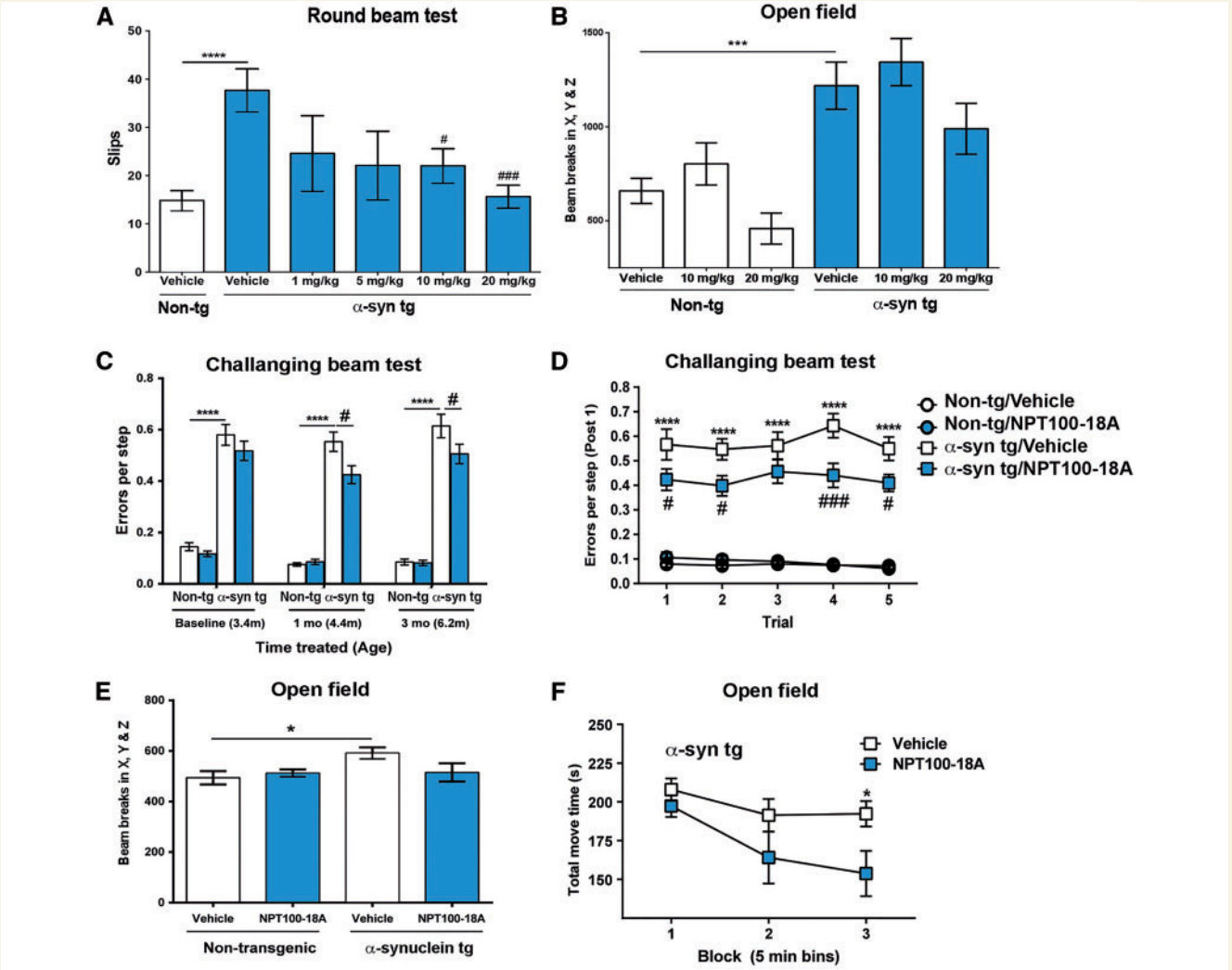

Figure 4 Effects of NPT100-18A on behavioural performance on α-synuclein transgenic mice at two independent sites. Comparable groups of mThy1-α-syn were treated for 3 months with vehicle (saline) or NPT100-18A at UCSD (**A** and **B**) and UCLA (**C–F**) and tested in the evaluations of motor behaviour in beam and open field tests. (**A**) Evaluation of round beam performance test at UCSD**.** Compared to non-transgenic, the vehicle-treated α-synuclein transgenic (tg) mice displayed significant deficits in the round horizontal beam test (****$P < 0.0001$, when compared to vehicle-treated non-transgenic group)**.** Treatment with NPT100-18A ameliorated the deficits at 10 and 20 mg/kg ($^{\#}P < 0.05$, $^{\#\#\#}P < 0.01$ compared to vehicle-treated α-synuclein transgenic mice). (**B**) Evaluation of spontaneous locomotor activity (open field) at UCSD. α-Synuclein transgenic mice displayed increased total activity in the open field test compared to non-transgenic controls ($P < 0.001$), but no statistically significant effects of NPT100-18A were detected. (**C**) Longitudinal evaluation of challenging beam performance at UCLA**.** Compared to non-transgenic littermates, the vehicle-treated α-synuclein transgenic mice displayed significant deficits in the challenging (grid) beam test conducted at UCLA (**C**, errors per step, group averages of five trials, ****$P < 0.0001$ when compared to vehicle-treated non-transgenic group). NPT100-18A treatment (10 mg/kg) decreased α-synuclein transgenic error rates on the challenging beam in 4.4- (**C**, middle) and 6.2- (**C**, right) month-old mice after 1 month of treatment (errors per step, group averages of five trials, $^{\#}P < 0.05$ versus vehicle-treated α-synuclein transgenic group). (**D**) Analysis of UCLA evaluation of α-synuclein transgenic challenging beam performance at 4.4 months (after 1 month of treatment) demonstrated that vehicle (saline)-treated wild-type α-synuclein mice had a statistically significant increase in the error rate for all trials compared to non-transgenic vehicle-treated mice (****$P < 0.0001$). NPT100-18A-treated α-synuclein transgenic mice had a statistically significant reduction in error rates on Trials 2, 4, and 5 of 5 ($^{\#}P < 0.05$, $^{\#\#\#}P < 0.01$ compared to vehicle-treated α-synuclein transgenic mice). **(E** and **F)** Open field assessment of locomotor activity**.** There were no statistically significant effects of NPT100-18A on α-synuclein transgenic total move time in the open field locomotor test averaged over 15 min (**E**); however, NPT100-18A-treated α-synuclein transgenic showed habituation in the open field (**F**), with significantly decreased activity in the third time bin compared to vehicle-treated α-synuclein transgenic mice. Non-transgenic (vehicle $n = 21$ and NPT100-18A $n = 22$) and α-synuclein transgenic mice (vehicle $n = 22$ and NPT100-18A $n = 20$), all mice were 6.2-month-old males treated for 3 months with NPT100-18A or vehicle (saline). Error bars are SEM.

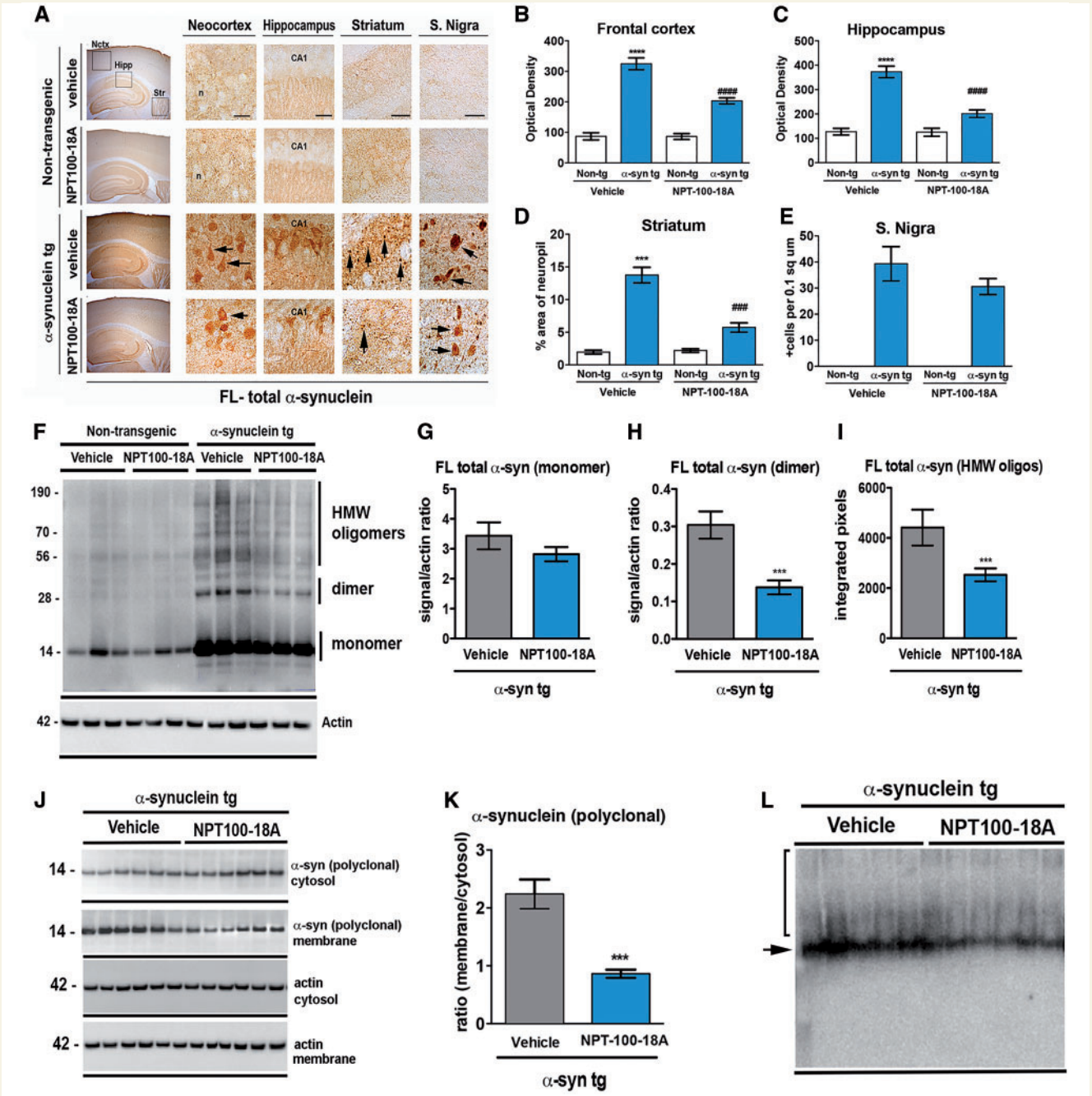

Figure 5 Immunocytochemical and western blot analysis of the effects of NPT100-18A on α-synuclein accumulation in transgenic mice. Groups of mThy1-wt-α-syn were treated for 3 months with vehicle or NPT100-18A at 20 mg/kg and analysed for levels of α-synuclein by immunocytochemistry and immunoblot. (**A**) Immunocytochemical analysis with a polyclonal antibody against full-length α-synuclein (FL). The column to the *left* is a low power view (20 ×) illustrating immunostaining of the neocortex (Nctx), hippocampus (Hipp) and striatum (Str) in each of the four groups analysed. The panels to the *right* illustrate a higher magnification view (630 ×) of the regions in open squares plus the substantia nigra. The images depict α-synuclein immunostaining of the neuropil in the non-transgenic mice and of the neuropil and neuropil and neuronal cells bodies (arrows) in the α-synuclein transgenic mice. (**B–E**) Computer aided image analysis of levels of α-synuclein in the frontal cortex, hippocampus, striatum and substantia nigra, respectively, showing greater accumulation of α-synuclein in the neuropil and cell bodies in the transgenic mice that were reduced with NPT100-18A treatment. (**F**) Immunoblot analysis with a polyclonal antibody against full-length α-synuclein with frontal cortex homogenates run on SDS-PAGE gels. In non-transgenic mice, a 14 kDa band that was primarily detected, while in the α-synuclein transgenic mice several bands corresponding to α-synuclein dimers and oligomers were detected. (**G**) Computer aided image analysis indicated that while the monomer was unaffected, the (**H**) dimer, and (**I**) higher molecular weight bands were significantly reduced by NPT100-18A in α-synuclein transgenic mice. (**J**) Immunoblot analysis with polyclonal antibodies against human α-synuclein with frontal cortex homogenates divided into cytosolic and membrane fractions run in SDS-PAGE gels. In vehicle-treated α-synuclein transgenic mice the 14 kDa band was more abundant in the membrane fraction, treatment with NPT100-18A shifted α-synuclein from the membrane (insoluble) to the cytosolic fraction

(continued)

confirmed by confocal microscopy analysis in double labelled sections with antibodies against C-terminus α-synuclein and neurofilaments (SMI312) (Supplementary Fig. 7C and D). As previous studies have shown that α-synuclein aggregates are proteinase K-resistant (Takeda *et al.*, 1998; Kahle *et al.*, 2001), additional immunocytochemical analysis was performed in sections pretreated with proteinase K. Following treatment (proteinase K +), α-synuclein immunoreactivity was similar to proteinase K− studies (Supplementary Fig. 7A and B) with extensive accumulation in the synapses and axonal processes in the vehicle-treated α-synuclein transgenic mice, which was reduced in the NPT100-18A-treated mice (Supplementary Fig. 7E and F). To visualize pathological α-synuclein, sections were immunostained with pSer129-α-syn antibody (Supplementary Fig. 7G); NPT100-18A significantly reduced the amount of immunoreactivity for pathological α-synuclein (Supplementary Fig. 7H).

Quantitative PCR analysis was performed to determine if the reduction in the levels of α-synuclein could be explained by effects of the drug at the mRNA levels. Increased levels of human *SNCA* were confirmed in the transgenic compared to the non-transgenic mice (Supplementary Fig. 8A), and levels of human *SNCA* mRNA were comparable in animals treated with NPT100-18A (Supplementary Fig. 8B). Levels of murine *Snca* were similar between the non-transgenic and transgenic groups (Supplementary Fig. 8C), and no effects of NPT100-18A were detected when compared to the vehicle groups (Supplementary Fig. 8D). Therefore, NPT100-18A effects are at the protein level and does not affect mRNA expression.

Taken together these studies suggest that in addition to functional motor performance improvements, NPT100-18A administration reduced accumulation of α-synuclein in synapses and axons in α-synuclein transgenic mice.

NPT100-18A ameliorated the neurodegenerative pathology in mThy1-α-syn wild-type transgenic mice

The effects of NPT100-18A administration on neurodegenerative pathology were evaluated in brain samples from the same study subjects described in the previous sections. Compared to non-transgenic mice, vehicle-treated α-synuclein transgenic mice displayed loss of NeuN-positive cells in the neocortex, CA3 region of the hippocampus, and striatum (Fig. 6A and B) accompanied by astrogliosis (increased GFAP levels) (Fig. 6A and C), loss of synaptophysin-positive nerve terminals (Fig. 6A and D), and MAP2-immunoreactive dendrites (Fig. 6A and E). Treatment with NPT100-18A treatment rescued the neuronal loss, synapto-dendritic pathology, and reduced astrogliosis in the neocortex, hippocampus, and striatum (Fig. 6A–E). Consistent with the confocal microscopy studies, ultrastructural analysis showed a reduction in the numbers of the presynaptic terminals in α-synuclein transgenic mice compared to non-transgenic mice, and these alterations were rescued in transgenic mice treated with NPT100-18A (Supplementary Fig. 9A and C). Immunogold analysis with an antibody against human α-synuclein showed extensive accumulation of gold particles in synapses and dendrites in the vehicle-treated α-synuclein transgenic mice. Animals treated with NPT100-18A displayed a significant reduction in the accumulation of α-synuclein in the nerve terminals (Supplementary Fig. 9B and D).

Compared to vehicle-treated non-transgenic mice, the α-synuclein transgenic mice showed a loss of TH-positive fibres in the striatum (Fig. 6F and G); however, no neuronal loss was detected in the substantia nigra. Treatment with NPT100-18A ameliorated the loss of TH-positive fibres in the striatum (Fig. 6F and G). In conclusion, improved behavioural performance in mice treated with NPT100-18A was associated with amelioration of α-synuclein pathology and the neurodegenerative phenotype present in α-synuclein transgenic mice.

NPT100-18A reduced the accumulation of oligomers and related synaptic deficits in mThy1-α-syn E57K transgenic mice

To further investigate the effects of the compound on α-synuclein oligomer formation in an alternate model, mThy1-α-syn E57K transgenic mice were treated with NPT100-18A (20 mg/kg). We have previously shown that this artificial mutation favours the formation if neurotoxic annular α-synuclein oligomers in the synapses and no fibrils are formed (Winner *et al.*, 2011; Rockenstein *et al.*, 2014). By immunoblot, vehicle-treated α-synuclein E57K transgenic mice displayed multimeric α-synuclein forms including dimers, trimers and higher order oligomers (Fig. 7A and B). Treatment with

Figure 5 Continued

(soluble). (**K**) Computer aided image analysis of a composite of α-synuclein in the membrane versus cytosolic fractions showing that NPT100-18A increased cytosolic α-synuclein while decreasing α-synuclein in the membrane fraction. (**L**) Immunoblot analysis of a polyclonal antibody against full-length α-synuclein with frontal cortex homogenates run in native gels. A band (arrow) as well as a smear were detected in the α-synuclein transgenic mice. Non-transgenic (vehicle $n = 21$ and NPT100-18A $n = 22$) and α-synuclein transgenic mice (vehicle $n = 22$ and NPT100-18A $n = 20$), all 3-month-old males treated for 3 months with NPT100-18A. $^{***}P < 0.05$ versus non-transgenic mice by one-way ANOVA with *post hoc* comparisons via Dunnett's; $^{\#\#\#}P < 0.05$ versus vehicle-treated α-synuclein transgenic mice by one-way ANOVA with *post hoc* comparisons via Tukey-Kramer. Error bars are SEM.

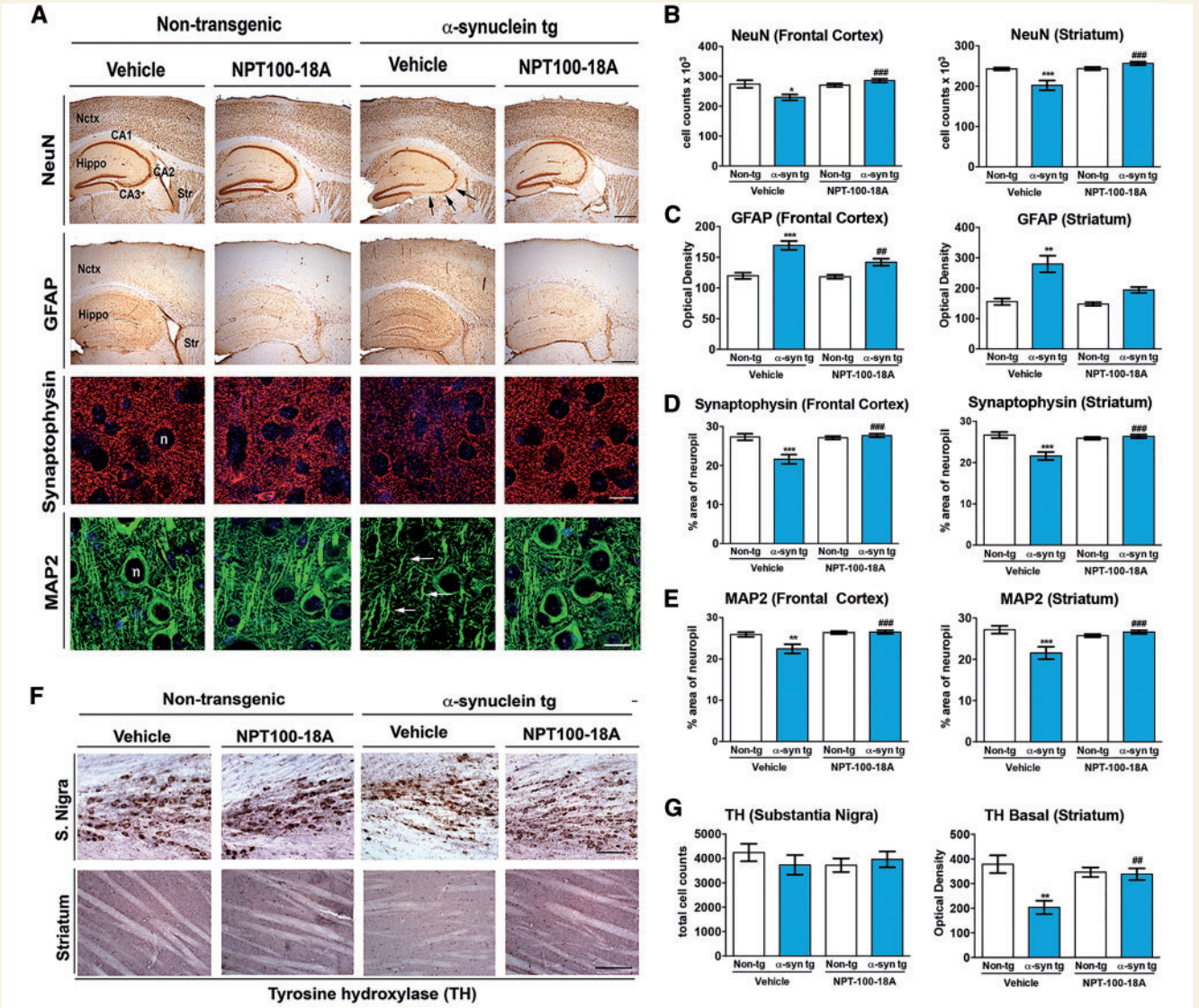

Figure 6 Neuropathological analysis of the effects of NPT100-18A on neurodegeneration in α-synuclein transgenic mice. Groups of mThy1-wt-α-syn were treated for 3 months with vehicle or NPT100-18A at 20 mg/kg and were analysed by immunocytochemistry for markers of neurodegeneration. (**A**) The *top two rows* are representative images at low power (20 ×) for sections immunostained with a neuronal (NeuN) and an astroglial cell marker (GFAP) reacted with diaminobenzidine and imaged with a digital bright field video microscope. The *bottom two rows* are representative images at higher power (900 ×) for sections immunostained with a presynaptic (synaptophysin) and a dendritic marker (MAP2) visualized with tyramide red and FITC, respectively, and imaged with a laser scanning confocal microscope. (**B**) Stereological analysis of NeuN positive cells in the frontal cortex and striatum showing reduced numbers in vehicle α-synuclein transgenic mice, which were recovered with NPT100-18A. (**C**) Densitometrical analysis of levels of GFAP immunoreactivity in the frontal cortex and striatum showing increased levels in vehicle α-synuclein transgenic mice and recovery with NPT100-18A. (**D** and **E**) Computer aided image analysis of the per cent area of the neuropil for synaptophysin (red) and MAP2 (green), respectively, in the frontal cortex and striatum showing decreased levels in vehicle α-synuclein transgenic mice and recovery with NPT100-18A. Arrows indicate damaged dendritic processes, *n* = nucleus. (**F**) The *top row* shows representative images at low power (20 ×) of the substantia nigra immunostained with an antibody against TH. The *bottom row* shows representative images at higher power (240 ×) of the striatum reacted with diaminobenzidine and imaged with a digital bright field video microscope. (**G**) Stereological counts of TH neurons in the substantia nigra (hemibrain). Densitometric analysis of TH fibres in the striatum showing decrease levels in vehicle α-synuclein transgenic mice and recovery with NPT100-18A. $^{*}P < 0.05$; $^{**}P < 0.01$; $^{***}P < 0.001$ versus non-transgenic mice by one way ANOVA with *post hoc* Dunnett's; $^{\#}P < 0.05$; $^{\#\#}P < 0.01$; $^{\#\#\#}P < 0.05$ versus vehicle-treated α-synuclein transgenic mice by one-way ANOVA with *post hoc* Tukey-Kramer. Non-transgenic vehicle ($n = 24$), non-transgenic NPT100-18A (20 mg/kg, $n = 17$), α-synuclein transgenic vehicle ($n = 20$), α-synuclein transgenic 20 mg/kg ($n = 13$). Scale bars: low magnification bar = 250 μm and high magnification bar = 25 μm. Error bars are SEM.

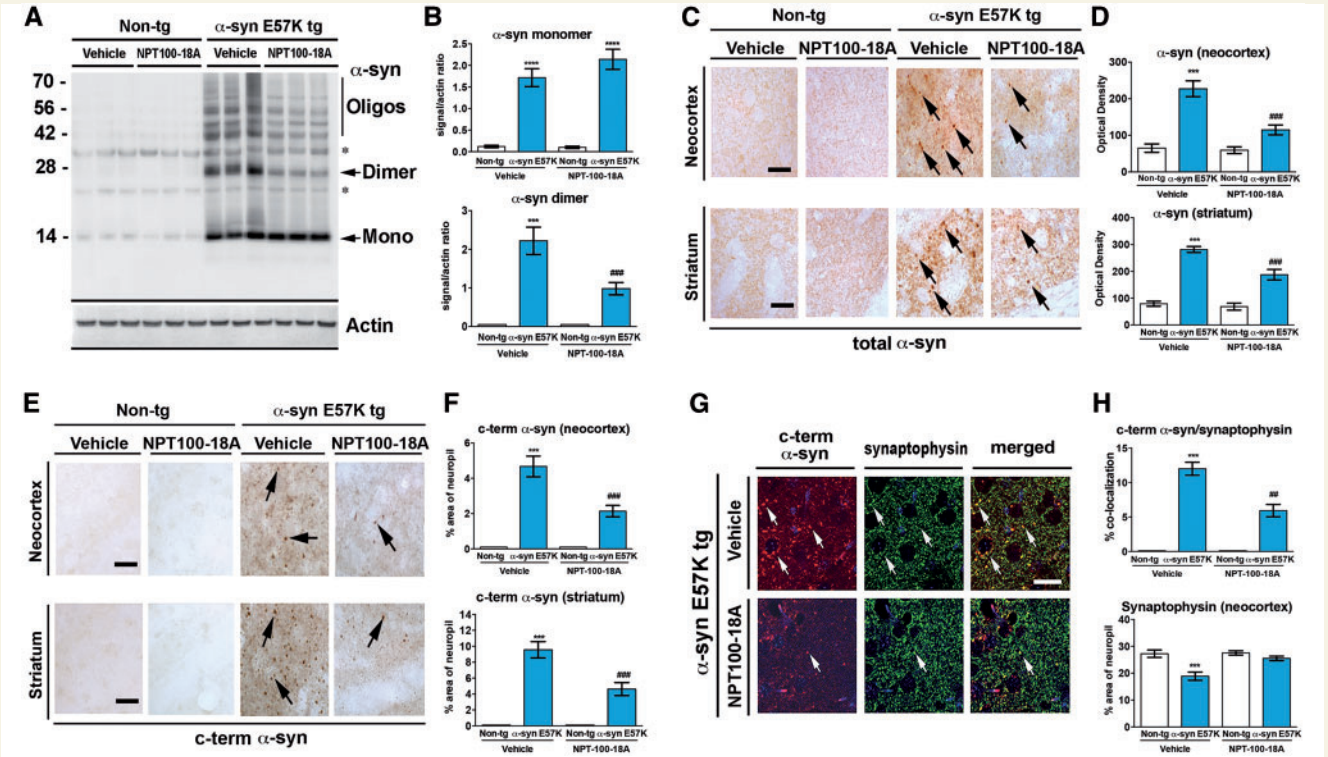

Figure 7 Immunoblot and immunocytochemical analysis of the effects of NPT100-18A on oligomer prone E57K α-synuclein transgenic mice. Groups of mThy1-E57K- α-synuclein transgenic mice were treated for 3 months with vehicle or NPT100-18A at 20 mg/kg and analysed by western blot and immunocytochemistry. (**A**) Immunoblot analysis with a polyclonal antibody against full-length α-synuclein with frontal cortex homogenates ran in SDS-PAGE gel, E57K α-synuclein transgenic mice show the presence of several bands between 28 to 70 kDa corresponding to α-synuclein multimers (oligomers). (**B**) Computer aided image analysis of the monomer and higher molecular weight bands showing that NPT100-18A reduced dimer in α-synuclein transgenic mice but had no effects on monomer levels. (**C**) Immunocytochemical analysis with a polyclonal antibody against full-length α-synuclein showing representative images illustrating immunostaining of the neocortex (Nctx) and striatum (Str) in the each of the four groups analysed at a high magnification view (630 ×). The images depict α-synuclein immunostaining of the neuropil in the non-transgenic mice and of the neuropil and dystrophic neurites (arrows). (**D**) Computer aided image analysis of levels of α-synuclein in the frontal cortex, and striatum showing greater accumulation of α-synuclein in the neuropil in the transgenic mice that was reduced with NPT100-18A treatment. (**E**) Immunocytochemical analysis with a monoclonal antibody against truncated α-synuclein; the column to the *left* is a low power view (20 ×), and the panels to the *right* are higher magnification view (630 ×). The E57K α-synuclein transgenic mice display strong immunostaining in the neuropil and dystrophic neurites (arrows). (**F**) Computer aided image analysis of levels of C-terminus truncated α-synuclein in the frontal cortex, and striatum showing greater accumulation of α-synuclein in the neuropil in the transgenic mice that is reduced with NPT100-18A treatment. (**G**) Double labelling with antibodies against C-terminus truncated α-synuclein (red) and the synaptic marker synaptophysin (green) and imaged with the laser scanning microscope. Arrows indicate co-localization between the two markers. (**H**) Image analysis of the per cent of synaptophysin terminals containing C-terminus truncated α-synuclein showing greater accumulation of α-synuclein in synapses in the transgenic mice that is reduced with NPT100-18A treatment. $^{***}P < 0.05$ versus non-transgenic mice by one-way ANOVA with *post hoc* Dunnett's. $^{\#\#\#}P < 0.05$ versus vehicle-treated α-synuclein transgenic mice by one-way ANOVA with *post hoc* Tukey-Kramer. Non-transgenic vehicle (n = 12), non-transgenic NPT100-18A (20 mg/kg, n = 12), α-synuclein transgenic vehicle (n = 12), α-synuclein transgenic 20 mg/kg (n = 12). Error bars are SEM. Scale bar = 15 μm.

NPT100-18A reduced α-synuclein dimers and other oligomers but had no effect on the monomers (Fig. 7A and B). Antibodies against total α-synuclein (Fig. 7C and D) and C-terminus α-synuclein (SYN105) (Fig. 7E and F) detected extensive accumulation of α-synuclein in synapses and axons in the neocortex and striatum of the vehicle α-synuclein E57K transgenic mice. Treatment with NPT100-18A significantly reduced the accumulation of total (Fig. 7C and D) and aggregated C-terminus α-synuclein (Fig. 7E and F) in the neuropil of the α-synuclein E57K transgenic mice. Accumulation of C-terminus α-synuclein in the synapses resulted in reduced synaptophysin localization to the terminals (Fig. 7G and H). Treatment with NPT100-18A led to decreased accumulation of α-synuclein in the terminals and rescued the loss of synaptophysin in the terminals (Fig. 7G and H). Taken together, these studies demonstrate that NPT100-18A treatment reduced accumulation of α-synuclein oligomers in the synapses allowing proper synaptophysin and vesicle localization to the terminals.

Live imaging using two-photon microscope shows NPT100-18A rapidly reduces α-synuclein in PDGF-α-syn-GFP transgenic mice

NPT100-18A administration produced beneficial effects on motor performance (Fig. 4) and structural effects at the synaptic level in transgenic mouse models (Fig. 6) in the absence of sustained brain levels of NPT100-18A, this suggested that NPT100-18A has a rapid but long lasting effect extending beyond the short-lived concentration of the compound in the brain. For this purpose we investigated in real time the temporally-varying influence of NPT100-18A by two-photon microscopy in PDGF-α-syn-GFP transgenic mice. We have previously shown that α-synuclein content in the synapses of these mice can be monitored over an extended period of time and is sensitive to the effects of molecules that regulate protein clearance (Unni *et al.*, 2010).

The α-syn-GFP construct in the α-syn-GFP transgenic mouse is stable and co-localizes with synaptic markers to the nerve terminals (Rockenstein *et al.*, 2005). Live imaging of vehicle-treated mice demonstrated the presence of abundant GFP-positive punctae-like terminals throughout the neuropil in the superficial layers of the neocortex (Fig. 8A). Monitoring synapses every 15 min for over 4 h showed that the levels of pixel intensity and terminal size were constant (Fig. 8B). The animals were first imaged under baseline conditions for 15 min and then NPT100-18A was administered intra-arterially (Fig. 8C). Synapse monitoring in these animals showed that levels of pixel intensity in ~75% of the synapses started to decrease between 30 to 60 min and then remained low for the rest of the imaging, the remaining 25% of the particles displayed constantly high levels of pixel intensity throughout the imaging protocol (Fig. 8D). This was consistently observed for the various cohorts of animals analysed.

To evaluate structural effects at the synaptic level in a transgenic mouse model using live imaging, a second cohort of α-syn-GFP transgenic mice were treated for 4 weeks with NPT100-18A and imaged the day after the last injection. Analysis of the particle size showed that in the NPT100-18A-treatment resulted in a reduction of the smallest particle size, and slight increase in the intermediate particle size compared to vehicle-treated mice (Fig. 8E and F). These studies suggest that treatment with NPT100-18A might reduce α-synuclein in the synapses and facilitate the clearance of α-synuclein.

These studies suggest NPT100-18A treatment might reduce α-synuclein aggregate accumulation in synapses and facilitate α-synuclein clearance. Therefore, neuronal cells were infected with the same α-syn-GFP construct driven by a lentiviral vectors. Co-labelling experiments showed that α-synuclein immunolabelling coincided with α-syn-GFP and was present in the neuronal cell body and neuritic processes including beaded structures (Supplementary Fig. 10A and B). NPT100-18A treatment reduced levels of α-syn-GFP in a dose-dependent manner (Supplementary Fig. 10C and D). Inhibition of α-syn-GFP clearance with bafilomycin A1 (BafA1), a downstream autophagy blocker, or lactacystin, a proteasome blocker, completely blocked the effects of NPT100-18A, while 3-methyladenine (3-MA), an upstream autophagy blocker, only partially blocked NPT100-18A effects (Supplementary Fig. 10E and F). In contrast, co-treatment with rapamycin, an autophagy inducer, enhanced clearance of α-syn-GFP (Supplementary Fig. 10E and F). Taken together, these results support the possibility that NPT100-18A rapidly affects α-synuclein accumulation in synapses, subsequently enhancing clearance via autophagy or proteasome pathways.

Discussion

We showed that a *de novo in silico* designed iso-indole pyrimido pyrazine compound (NPT100-18A) prevented the formation of neurotoxic α-synuclein in neurons by potentially altering α-synuclein interactions in the membrane thereby reducing oligomer formation. Moreover, this compound ameliorated behavioural deficits and neurodegeneration in different models of synucleinopathies suggesting that targeting the displacement of α-synuclein from the membrane might be a viable treatment strategy for synucleinopathies.

Aggregated forms of α-synuclein can disrupt neuronal function and confer neurotoxicity to varying degrees by multiple mechanisms (Lashuel *et al.*, 2013; Stockl *et al.*, 2013). The mechanisms are under investigation; however, a study has shown that dopaminergic neurons may be selectively vulnerable to degeneration in Parkinson's disease due to cytosolic dopamine promoting the accumulation of toxic α-synuclein protofibrils (Rochet *et al.*, 2004). Thus the development of therapeutic agents that intervene with this process has become a compelling novel approach to the treatment of Parkinson's disease and related disorders. We focused on the process of α-synuclein displacement from the membrane since previous studies suggests that conversion of α-synuclein into propagating homodimers on the membrane might be the initial step leading to formation of oligomers of various sizes (Tsigelny *et al.*, 2012; Roostaee *et al.*, 2013). Supporting a role of dimerization in synucleinopathies, *in vitro* studies have shown the presence of a dimeric state during conversion of α-synuclein from soluble monomers to oligomeric toxic species (Roostaee *et al.*, 2013). Dimer formation and subsequent toxic aggregation of wild-type α-synuclein can be induced by environmental oxidative stress conditions (Fernagut *et al.*, 2007) leading to cross-linking of tyrosine residues (Hashimoto *et al.*, 1998; Krishnan *et al.*, 2003). Artificial introduction of α-synuclein mutations that reduce interactions with lipid membranes results in decreased oligomer formation and abrogate neurotoxicity (Ysselstein *et al.*,

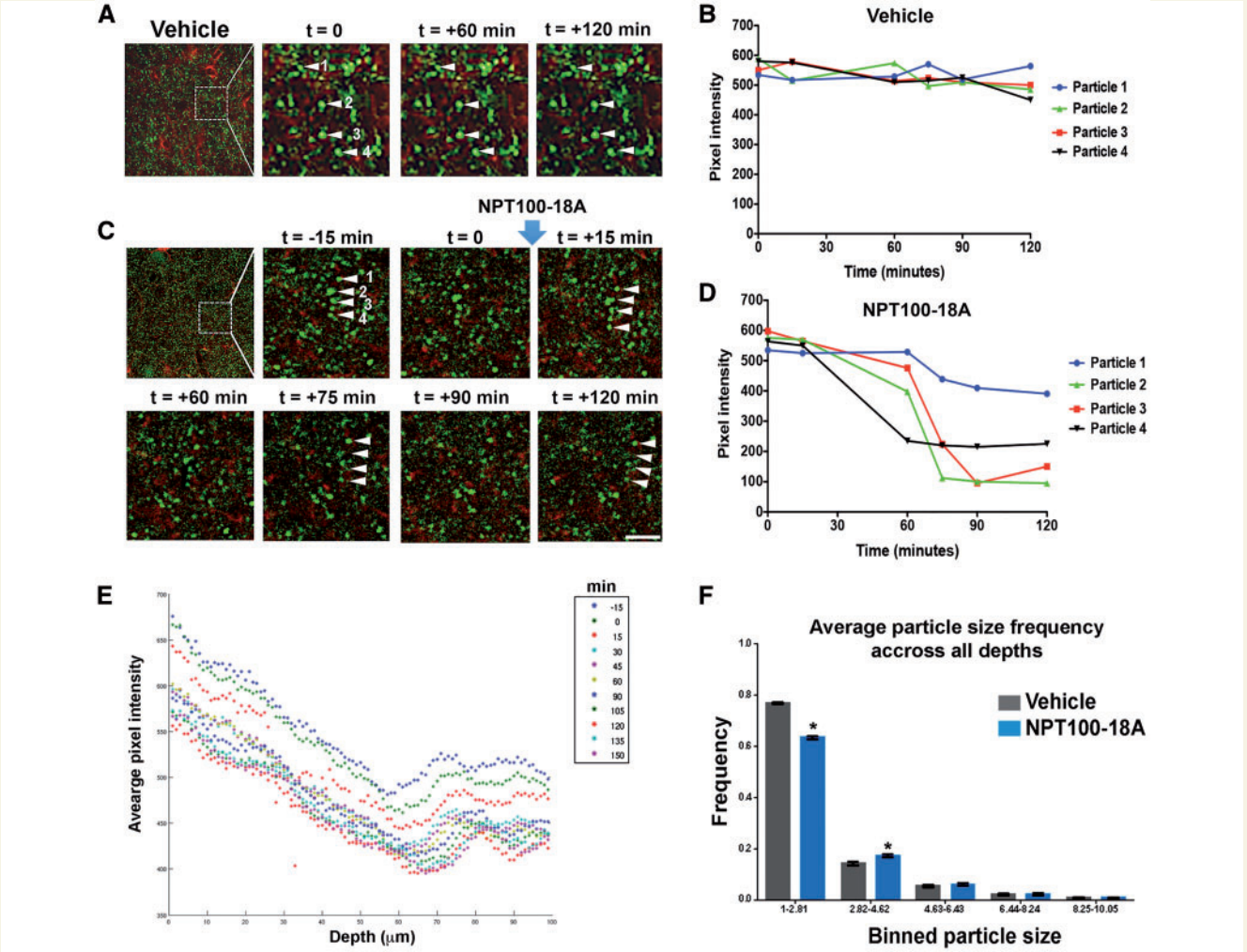

Figure 8 Two-photon live imaging of the effects of NPT100-18A on α-synuclein accumulation in synapses in α-syn-GFP transgenic mice. Groups of α-syn-GFP transgenic mice were anaesthetized, a window was opened in the skull, and the neocortex was imaged for a period of over 2 h with a two-photon microscope. (**A**) Acute evaluation of vehicle-treated α-syn-GFP transgenic mice, the punctae (green, arrowheads) represent individual synaptic terminals containing α-synuclein. The brains were counter-stained with the glial marker SR101 (red). (**B**) Computer aided image analysis of presynaptic terminals (numbered arrowheads) over time showing the levels of fluorescence were stable. (**C**) NPT100-18A-treated α-syn-GFP transgenic mice, the punctae (green, arrowheads) represent individual synaptic terminals containing α-synuclein, the brains were counter-stained with the glial marker SR101 (red). Over time, following acute NPT100-18A treatment (time = 0 min), the levels decrease in some of terminals. (**D**) Computer aided image analysis of α-syn-GFP terminals (numbered arrowheads) over time showing the decay in levels of fluorescence following NPT100-18A. (**E**) Data from a representative animal showing fluorescence levels decreasing with time from 15 min before treatment to 150 min post-treatment across depth up to 100 μm. Fluorescence levels naturally decrease with increasing depth despite increasing the laser power since there is more tissue above the focal plane. (**F**) Particle size analysis in chronically treated mice. Binning of particle data (in this case the particle is GFP α-synuclein in nerve terminals) was performed to characterize a statistical distribution of particle size. NPT100-18A decreased the number of particles in the smallest bin. A total of 12 transgenic mice (6 months old, $n = 6$ vehicle and $n = 6$ NPT100-18A) were used; error bars are SEM. *$P < 0.05$ versus the respective binned particle size group for vehicle treated mice by one-way ANOVA followed by Dunnett's *post hoc* analysis.

2015) supporting the view that reducing membrane binding and homodimer formation might prevent the formation of neurotoxic α-synuclein oligomers.

However, not all α-synuclein mutations lead to aggregation and toxicity via membrane interactions. For example, the familial A30P and G51D mutations display lower affinity to the membrane, also result in α-synuclein aggregation and toxicity (Ysselstein *et al.*, 2015). Moreover, a recent study showed that artificial point mutations that inhibit vesicle membrane binding were associated with aggregation and toxicity (Burre *et al.*, 2015). In healthy synapses α-synuclein is present in equilibrium between a cytosolic monomer that is natively unfolded and a vesicle membrane-bound form that is a tetramer (Bartels *et al.*, 2011) and chaperones the SNARE complex (Burre *et al.*, 2015). There is some controversy in the field: whether α-synuclein

tetramers have a functional role in the membranes; and which species are toxic. It is possible that there are multiple conformations of α-synuclein dimers, tetramers, and higher order multimers for which some might have a functional role and other conformations might be toxic (Tsigelny *et al.*, 2015). Under normal conditions α-synuclein binding to vesicle membranes is hypothesized to stabilize α-synuclein into a conformation that is unavailable for binding to other cellular membranes. If such interactions do not occur, the soluble α-synuclein is free to interact with other cellular membranes. Our study, as well as other studies, have investigated α-synuclein toxic oligomers in the membrane, α-synuclein interactions with the plasma (Tsigelny *et al.*, 2015), endoplasmic reticulum (Colla *et al.*, 2012), and mitochondrial membranes (Nakamura *et al.*, 2011). Therefore, one possibility is that NPT100-18A might work by displacing α-synuclein from plasma and other intracellular organelles, but it might not alter the physiological α-synuclein associated with synaptic vesicles. In whole homogenates under reducing conditions we observe reduced accumulation of α-synuclein oligomers. While in cytosolic versus membrane fraction we observe a reduction in the membranes. This might be explained by reducing the load of aggregated α-synuclein and facilitate the clearance of α-synuclein from the membrane including in monomeric species. In native gels we observed a reduction of higher molecular weight α-synuclein. Further evaluation of this hypothesis is needed.

Various therapeutic strategies for targeting α-synuclein range from anti-amyloid agents that disrupt the large intracellular fibrils, to those targeting the cell-to-cell propagation of misfolded oligomeric aggregates, or those that target the fibril growth phase as modelled by the addition of monomeric α-synuclein to protofibril 'seeds' (Lashuel *et al.*, 2013). The present approach is novel in that we aim to intervene at early stages of this process by preventing the initial formation of membrane-embedded dimers or smaller α-synuclein oligomers. Targeting the initial formation of the membrane-embedded oligomeric α-synuclein could prevent the formation of both the smaller toxic oligomeric α-synuclein, as well as larger downstream protofibrils without necessarily interfering with the physiological functions of α-synuclein. Disrupting the formation of membrane-embedded dimers at this early intervention point could reverse the adverse effects of α-synuclein on synaptic function at a stage before irreversible neurodegenerative processes have been initiated. Finally, specifically targeting the α-synuclein structure that is stabilized in cell membranes allows for a more specific molecularly targeted drug design. Supporting this mechanism, the molecular simulations and NMR studies suggest the possibility that NPT100-18A displaced α-synuclein from the membrane, consequently reducing α-synuclein toxic conversion to propagating dimers and oligomers. Likewise electron microscopy studies demonstrated that NPT100-18A reduced the formation of globular oligomers in a lipid membrane matrix. Remarkably, since the E83 residue of α-synuclein interacts with the H-bond donor groups of NPT100-18A, substitution of this residue for arginine abrogated the effects of compound to block α-synuclein toxic conversion, suggests the beneficial effects of NPT100-18A were related to its ability to displace α-synuclein from the membrane.

While we used molecular dynamic simulations to develop *de novo* a compound that attenuates α-synuclein interaction with lipids at early stages of the oligomerization process, other studies have used different approaches including high-throughput screening to identify oligomer modulator compounds (El-Agnaf *et al.*, 2004; Wagner *et al.*, 2013) including baicalein (Lu *et al.*, 2011), curcumin (Pandey *et al.*, 2008), and gallic acid (3,4,5-trihydroxybenzoic acid) (Ardah *et al.*, 2014). Other compounds that reduce α-synuclein oligomerization and toxicity include SNX-0723 (Putcha *et al.*, 2010), mannitol (Shaltiel-Karyo *et al.*, 2013), and AT2101 (Richter *et al.*, 2014). Taken together, these studies support the hypothesis that interfering at various stages with the process of α-synuclein aggregation might be beneficial. However, it is worth noting that several of the approaches reviewed above not only reduce α-synuclein aggregation but also might non-selectively interfere with amyloid-β, PrP and tau. The NPT100-18A compound differs in that it was designed to more selectively target the folded state of α-synuclein in the membrane. Additional studies are needed to understand the complex effects of NPT100-18A on physiological tetramers verses pathological α-synuclein monomer and oligomers.

Considering α/β-synuclein concentration at the synapse is thought to be ~40 μM (Wilhelm *et al.*, 2014), then in theory one would need a working NPT100-18A concentration of ~200 μM. However, despite the finding that NPT100-18A had a relatively short half-life in the brain and modest brain penetration, considerable effects were observed *in vivo*, including those with the two-photon microscope that detected a rapid effect of the compound on α-synuclein in synapses. Although there is a large pool of α-synuclein in the CNS, the proportion prone to aggregate into oligomers is relatively small (Lee *et al.*, 2005; Danzer *et al.*, 2007; Sandal *et al.*, 2008), and conditions such as propagation and defects in clearance mechanisms might amplify the accumulation of pathological of α-synuclein. Consequently, NPT100-18A might facilitate or synergize the clearance of misfolded α-synuclein and accumulation of α-synuclein on the membrane with catalytic-like effects even when the concentration of NPT100-18A is in the nanomolar range in the brain. Supporting this possibility, we observed that inhibitors of the proteasome and autophagy abrogate the effects of NPT100-18A, it is possible that while aggregated and oligomeric α-synuclein is cleared via the lysosme, monomeric α-synuclein might be cleared through the proteasome (Alvarez-Castelao *et al.*, 2014). Additional experiments will be needed to explore these mechanisms.

In conclusion, targeting α-synuclein oligomerization with small molecules might represent a potential approach for

developing treatments for Parkinson's disease and other synucleinopathies.

Acknowledgements

The authors thank B. Boodaie and H. Baker for their assistance with behavioural studies at UCLA.

Funding

This work was supported by a grant from the National Institute of Aging of the National Institutes of Health under award number R37AG018440 and a lab services agreement with Neuropore Therapies Inc to E.M., as well as a award from The Michael J. Fox Foundation to E.M. and Neuropore Therapies Inc. The data were analyzed and the manuscript written independent of company interests. The content is solely the responsibility of the authors and does not necessarily represent the official views of the National Institutes of Health.

Supplementary material

Supplementary material is available at *Brain* online.

References

Alvarez-Castelao B, Goethals M, Vandekerckhove J, Castano JG. Mechanism of cleavage of alpha-synuclein by the 20S proteasome and modulation of its degradation by the RedOx state of the N-terminal methionines. Biochim Biophys Acta 2014; 1843: 352–65.

Ardah MT, Paleologou KE, Lv G, Abul Khair SB, Kazim AS, Minhas ST, et al. Structure activity relationship of phenolic acid inhibitors of alpha-synuclein fibril formation and toxicity. Front Aging Neurosci 2014; 6: 197.

Bar-On P, Crews L, Koob AO, Mizuno H, Adame A, Spencer B, et al. Statins reduce neuronal alpha-synuclein aggregation in in vitro models of Parkinson's disease. J Neurochem 2008; 105: 1656–67.

Bartels T, Choi JG, Selkoe DJ. α-Synuclein occurs physiologically as a helically folded tetramer that resists aggregation. Nature 2011; 477: 107–10.

Beyer K. Mechanistic aspects of Parkinson's disease: alpha-synuclein and the biomembrane. Cell Biochem Biophys 2007; 47: 285–99.

Bortolus M, Tombolato F, Tessari I, Bisaglia M, Mammi S, Bubacco L, et al. Broken helix in vesicle and micelle-bound alpha-synuclein: insights from site-directed spin labeling-EPR experiments and MD simulations. J Am Chem Soc 2008; 130: 6690–1.

Brundin P, Melki R, Kopito R. Prion-like transmission of protein aggregates in neurodegenerative diseases. Nat Rev Mol Cell Biol 2010; 11: 301–7.

Bucciantini M, Giannoni E, Chiti F, Baroni F, Formigli L, Zurdo J, et al. Inherent toxicity of aggregates implies a common mechanism for protein misfolding diseases. Nature 2002; 416: 507–11.

Burre J, Sharma M, Sudhof TC. Definition of a molecular pathway mediating alpha-synuclein neurotoxicity. J Neurosci 2015; 35: 5221–32.

Cavanagh J, Palmer AG, Wright PE, Rance M. Sensitivity improvement in proton-detected 2-dimensional heteronuclear relay spectroscopy. J Magn Reson 1991; 91: 429–36.

Colla E, Jensen PH, Pletnikova O, Troncoso JC, Glabe C, Lee MK. Accumulation of toxic alpha-synuclein oligomer within endoplasmic reticulum occurs in alpha-synucleinopathy *in vivo*. J Neurosci 2012; 32: 3301–5.

Conway KA, Lee SJ, Rochet JC, Ding TT, Williamson RE, Lansbury PT, Jr. Acceleration of oligomerization, not fibrillization, is a shared property of both alpha-synuclein mutations linked to early-onset Parkinson's disease: implications for pathogenesis and therapy. Proc Natl Acad Sci USA 2000; 97: 571–6.

Cremades N, Cohen SI, Deas E, Abramov AY, Chen AY, Orte A, et al. Direct observation of the interconversion of normal and toxic forms of alpha-synuclein. Cell 2012; 149: 1048–59.

Crews L, Spencer B, Desplats P, Patrick C, Paulino A, Rockenstein E, et al. Selective molecular alterations in the autophagy pathway in patients with Lewy body disease and in models of alpha-synucleinopathy. PLoS One 2010; 5: e9313.

Danzer KM, Haasen D, Karow AR, Moussaud S, Habeck M, Giese A, et al. Different species of alpha-synuclein oligomers induce calcium influx and seeding. J Neurosci 2007; 27: 9220–32.

Dehay B, Martinez-Vicente M, Caldwell GA, Caldwell KA, Yue Z, Cookson MR, et al. Lysosomal impairment in Parkinson's disease. Mov Disord 2013; 28: 725–32.

Delaglio F, Grzesiek S, Vuister GW, Zhu G, Pfeifer J, Bax A. NMRPipe: a multidimensional spectral processing system based on UNIX pipes. J Biomol NMR 1995; 6: 277–93.

El-Agnaf OM, Paleologou KE, Greer B, Abogrein AM, King JE, Salem SA, et al. A strategy for designing inhibitors of alpha-synuclein aggregation and toxicity as a novel treatment for Parkinson's disease and related disorders. FASEB J 2004; 18: 1315–7.

Eleuteri S, Di Giovanni S, Rockenstein E, Mante M, Adame A, Trejo M, et al. Novel therapeutic strategy for neurodegeneration by blocking Abeta seeding mediated aggregation in models of Alzheimer's disease. Neurobiol Dis 2015; 74: 144–57.

Farrer M, Maraganore DM, Lockhart P, Singleton A, Lesnick TG, de Andrade M, et al. alpha-Synuclein gene haplotypes are associated with Parkinson's disease. Hum Mol Genet 2001; 10: 1847–51.

Fernagut PO, Hutson CB, Fleming SM, Tetreaut NA, Salcedo J, Masliah E, et al. Behavioral and histopathological consequences of paraquat intoxication in mice: effects of alpha-synuclein overexpression. Synapse 2007; 61: 991–1001.

Ford MG, Pearse BM, Higgins MK, Vallis Y, Owen DJ, Gibson A, et al. Simultaneous binding of PtdIns(4,5)P2 and clathrin by AP180 in the nucleation of clathrin lattices on membranes. Science 2001; 291: 1051–5.

Fujioka S, Ogaki K, Tacik PM, Uitti RJ, Ross OA, Wszolek ZK. Update on novel familial forms of Parkinson's disease and multiple system atrophy. Parkinsonism Relat Disord 2014; 20 (Suppl 1): S29–34.

Games D, Seubert P, Rockenstein E, Patrick C, Trejo M, Ubhi K, et al. Axonopathy in an alpha-synuclein transgenic model of Lewy body disease is associated with extensive accumulation of C-terminal-truncated alpha-synuclein. Am J Pathol 2013; 182: 940–53.

Hashimoto M, Hernandez-Ruiz S, Hsu L, Sisk A, Xia Y, Takeda A, et al. Human recombinant NACP/a-synuclein is aggregated and fibrillated in vitro: relevance for Lewy body disease. Brain Res 1998; 799: 301–6.

Kahle PJ, Neumann M, Ozmen L, Muller V, Odoy S, Okamoto N, et al. Selective insolubility of alpha-synuclein in human Lewy body diseases is recapitulated in a transgenic mouse model. Am J Pathol 2001; 159: 2215–25.

Kay LE, Keifer P, Saarinen T. Pure absorption gradient enhanced heteronuclear single quantum correlation spectroscopy with improved sensitivity. J Am Chem Soc 1992; 114: 10663–5.

Krishnan S, Chi EY, Wood SJ, Kendrick BS, Li C, Garzon-Rodriguez W, et al. Oxidative dimer formation is the critical rate-limiting step for Parkinson's disease alpha-synuclein fibrillogenesis. Biochemistry 2003; 42: 829–37.

Kruger R, Kuhn W, Muller T, Woitalla D, Graeber M, Kosel S, et al. Ala30Pro mutation in the gene encoding alpha-synuclein in Parkinson's disease. Nat Genet 1998; 18: 106–8.

Lashuel HA, Hartley D, Petre BM, Walz T, Lansbury PT, Jr. Neurodegenerative disease: amyloid pores from pathogenic mutations. Nature 2002; 418: 291.

Lashuel HA, Overk CR, Oueslati A, Masliah E. The many faces of alpha-synuclein: from structure and toxicity to therapeutic target. Nat Rev Neurosci 2013; 14: 38–48.

Lee HJ, Patel S, Lee SJ. Intravesicular localization and exocytosis of alpha-synuclein and its aggregates. J Neurosci 2005; 25: 6016–24.

Lee SJ, Desplats P, Sigurdson C, Tsigelny I, Masliah E. Cell-to-cell transmission of non-prion protein aggregates. Nat Rev Neurol 2010; 6: 702–6.

Lu JH, Ardah MT, Durairajan SS, Liu LF, Xie LX, Fong WF, et al. Baicalein inhibits formation of alpha-synuclein oligomers within living cells and prevents Abeta peptide fibrillation and oligomerisation. Chembiochem 2011; 12: 615–24.

Luk KC, Kehm VM, Zhang B, O'Brien P, Trojanowski JQ, Lee VM. Intracerebral inoculation of pathological alpha-synuclein initiates a rapidly progressive neurodegenerative alpha-synucleinopathy in mice. J Exp Med 2012; 209: 975–86.

Masliah E, Rockenstein E, Mante M, Crews L, Spencer B, Adame A, et al. Passive immunization reduces behavioral and neuropathological deficits in an alpha-synuclein transgenic model of Lewy body disease. PLoS One 2011; 6: e19338.McKeith IG, Dickson DW, Lowe J, Emre M, O'Brien JT, Feldman H, et al. Diagnosis and management of dementia with Lewy bodies: third report of the DLB Consortium. Neurology 2005; 65: 1863–72.

Nakamura K, Nemani VM, Azarbal F, Skibinski G, Levy JM, Egami K, et al. Direct membrane association drives mitochondrial fission by the Parkinson disease-associated protein alpha-synuclein. J Biol Chem 2011; 286: 20710–26.Pandey N, Strider J, Nolan WC, Yan SX, Galvin JE. Curcumin inhibits aggregation of alpha-synuclein. Acta Neuropathol 2008; 115: 479–89.

Polymeropoulos M, Lavedan C, Leroy E, Ide S, Dehejia A, Dutra A, et al. Mutation in the a-synuclein gene identified in families with Parkinson's disease. Science 1997; 276: 2045–7.

Putcha P, Danzer KM, Kranich LR, Scott A, Silinski M, Mabbett S, et al. Brain-permeable small-molecule inhibitors of Hsp90 prevent alpha-synuclein oligomer formation and rescue alpha-synuclein-induced toxicity. J Pharmacol Exp Ther 2010; 332: 849–57.

Richter F, Fleming SM, Watson M, Lemesre V, Pellegrino L, Ranes B, et al. A GCase chaperone improves motor function in a mouse model of synucleinopathy. Neurotherapeutics 2014; 11: 840–56.

Rochet JC, Outeiro TF, Conway KA, Ding TT, Volles MJ, Lashuel HA, et al. Interactions among alpha-synuclein, dopamine, and biomembranes: some clues for understanding neurodegeneration in Parkinson's disease. J Mol Neurosci 2004; 23: 23–34.

Rockenstein E, Nuber S, Overk CR, Ubhi K, Mante M, Patrick C, et al. Accumulation of oligomer-prone alpha-synuclein exacerbates synaptic and neuronal degeneration in vivo. Brain 2014; 137 (Pt 5): 1496–513.

Rockenstein E, Schwach G, Ingolic E, Adame A, Crews L, Mante M, et al. Lysosomal pathology associated with alpha-synuclein accumulation in transgenic models using an eGFP fusion protein. J Neurosci Res 2005; 80: 247–59.

Roostaee A, Beaudoin S, Staskevicius A, Roucou X. Aggregation and neurotoxicity of recombinant alpha-synuclein aggregates initiated by dimerization. Mol Neurodegener 2013; 8: 5.

Sandal M, Valle F, Tessari I, Mammi S, Bergantino E, Musiani F, et al. Conformational equilibria in monomeric alpha-synuclein at the single-molecule level. PLoS Biol 2008; 6: e6.

Shaltiel-Karyo R, Frenkel-Pinter M, Rockenstein E, Patrick C, Levy-Sakin M, Schiller A, et al. A blood-brain barrier (BBB) disrupter is also a potent alpha-synuclein (alpha-syn) aggregation inhibitor: a novel dual mechanism of mannitol for the treatment of Parkinson disease (PD). J Biol Chem 2013; 288: 17579–88.

Singleton AB, Farrer M, Johnson J, Singleton A, Hague S, Kachergus J, et al. alpha-Synuclein locus triplication causes Parkinson's disease. Science 2003; 302: 841.

Singleton AB, Farrer MJ, Bonifati V. The genetics of Parkinson's disease: progress and therapeutic implications. Mov Disord 2013; 28: 14–23.

Spencer B, Michael S, Shen J, Kosberg K, Rockenstein E, Patrick C, et al. Lentivirus mediated delivery of neurosin promotes clearance of wild-type alpha-synuclein and reduces the pathology in an alpha-synuclein model of LBD. Mol Ther 2013; 21: 31–41.

Spencer B, Potkar R, Trejo M, Rockenstein E, Patrick C, Gindi R, et al. Beclin 1 gene transfer activates autophagy and ameliorates the neurodegenerative pathology in alpha-synuclein models of Parkinson's and Lewy body diseases. J Neurosci 2009; 29: 13578–88.

Spillantini MG, Schmidt ML, Lee VM, Trojanowski JQ, Jakes R, Goedert M. Alpha-synuclein in Lewy bodies. Nature 1997; 388: 839–40.

Stockl MT, Zijlstra N, Subramaniam V. alpha-Synuclein oligomers: an amyloid pore? Insights into mechanisms of alpha-synuclein oligomer-lipid interactions. Mol Neurobiol 2013; 47: 613–21.

Takeda A, Hashimoto M, Mallory M, Sundsmo M, Hansen L, Sisk A, et al. Abnormal distribution of the non-Ab component of Alzheimer's disease amyloid precursor/a-synuclein in Lewy body disease as revealed by proteinase K and formic acid pretreatment. LabInvest 1998; 78: 1169–77.

Tan EK, Skipper LM. Pathogenic mutations in Parkinson disease. Hum Mutat 2007; 28: 641–53.

Tiscornia G, Singer O, Verma IM. Design and cloning of lentiviral vectors expressing small interfering RNAs. Nat Protoc 2006; 1: 234–40.

Toth G, Gardai SJ, Zago W, Bertoncini CW, Cremades N, Roy SL, et al. Targeting the intrinsically disordered structural ensemble of alpha-synuclein by small molecules as a potential therapeutic strategy for Parkinson's disease. PLoS One 2014; 9: e87133.

Tsigelny IF, Sharikov Y, Kouznetsova VL, Greenberg JP, Wrasidlo W, Overk C, et al. Molecular determinants of alpha-synuclein mutants' oligomerization and membrane interactions. ACS Chem Neurosci 2015; 6: 403–16.

Tsigelny IF, Sharikov Y, Miller MA, Masliah E. Mechanism of alpha-synuclein oligomerization and membrane interaction: theoretical approach to unstructured proteins studies. Nanomedicine 2008; 4: 350–7.

Tsigelny IF, Sharikov Y, Wrasidlo W, Gonzalez T, Desplats PA, Crews L, et al. Role of alpha-synuclein penetration into the membrane in the mechanisms of oligomer pore formation. FEBS J 2012; 279: 1000–13.

Unni VK, Weissman TA, Rockenstein E, Masliah E, McLean PJ, Hyman BT. In vivo imaging of alpha-synuclein in mouse cortex demonstrates stable expression and differential subcellular compartment mobility. PLoS One 2010; 5: e10589.

van Rooijen BD, Claessens MM, Subramaniam V. Membrane permeabilization by oligomeric alpha-synuclein: in search of the mechanism. PLoS One 2010; 5: e14292.

Wagner J, Ryazanov S, Leonov A, Levin J, Shi S, Schmidt F, et al. Anle138b: a novel oligomer modulator for disease-modifying therapy of neurodegenerative diseases such as prion and Parkinson's disease. Acta Neuropathol 2013; 125: 795–813.

Wakabayashi K, Hayashi S, Kakita A, Yamada M, Toyoshima Y, Yoshimoto M, et al. Accumulation of a-synuclein/NACP is a cytopathological feature common to Lewy body disease and multiple system atrophy. Acta Neuropathol 1998; 96: 445–52.

Wilhelm BG, Mandad S, Truckenbrodt S, Krohnert K, Schafer C, Rammner B, et al. Composition of isolated synaptic boutons reveals the amounts of vesicle trafficking proteins. Science 2014; 344: 1023–8.

Winner B, Jappelli R, Maji SK, Desplats PA, Boyer L, Aigner S, et al. In vivo demonstration that alpha-synuclein oligomers are toxic. Proc Natl Acad Sci USA 2011; 108: 4194–9.

Xilouri M, Brekk OR, Stefanis L. Autophagy and alpha-synuclein: relevance to parkinson's disease and related synucleopathies. Mov Disord 2016; 31: 178–92.

Ysselstein D, Joshi M, Mishra V, Griggs AM, Asiago JM, McCabe GP, et al. Effects of impaired membrane interactions on alpha-synuclein aggregation and neurotoxicity. Neurobiol Dis 2015; 79: 150–63.